UMEÅ UNIVERSITY MEDICAL DISSERTATIONS
New Series No 1180 – ISSN 0346-6612 – ISBN 978-91-7264-567-7

On dopamine neurons. Nerve fiber outgrowth and L-DOPA effects

Sara af Bjerkén

Umeå 2008

Department of Integrative Medical Biology, Section for Histology and Cell Biology, Umeå University, Umeå, Sweden

Department of Integrative Medical Biology
Section for Histology and Cell biology
Umeå University

Cover illustration: Photomicrograph of dopamine nerve fibers (red) and astrocytes (green) in mice fetal ventral mesencephalic slice culture.

ISSN: 0346-6612
ISBN: 978-91-7264-567-7
Printed in Sweden by Arkitektkopia, Umeå 2008

To my family

TABLE OF CONTENTS

ABBREVIATIONS

5-HT	5-hydroxytryptamine (serotonin)
6-OHDA	6-hydroxydopamine
AADC	L- aromatic amino acid decarboxylase
AIM	Abnormal involuntary movements
ALDH1	Aldehyde dehydrogenase-1
Ara-C	Cytosine β-D-arabinofuranoside
CNS	Central nervous system
CRL	Crown-rump length
DAPI	4',6-diamidino-2-phenylindole
DIV	Days *in vitro*
DMEM	Dulbecco's modified Eagle´s medium
E	Embryonic day
ELISA	Enzyme-linked immunosorbet assay
FCS	Fetal calf serum
GABA	Gamma-aminobutyric acid
GDNF	Glial cell line-derived neurotrophic factor
GFRα1	Glycosylphosphatidylinositol-linked co-receptor 1
GLAST	Glia glutamate transporter
GP	Globus Pallidus
GPe	Globus Pallidus pars externa
GPi	Globus Pallidus pars interna
HCl	Hydrochloric acid
i.p.	Intraperitoneal
LGE	Lateral ganglionic eminence
L-DOPA	3,4-dihydroxy-L-phenylalanine
NCAM	Neural cell adhesion molecule
PCR	Polymerase chain reaction
s.c.	Subcutaneous
SERT	Serotonin transporter
SN	Substantia nigra
SNc	Substantia nigra pars compacta
SNr	Substantia nigra pars reticulata
STN	Subthalamic nucleus
TH	Tyrosine Hydroxylase
VM	Ventral mesencephalon
VTA	Ventral tegmental area

ABSTRACT

Parkinson's disease is a disorder mainly characterized by progressive degeneration of dopamine producing neurons in the substantia nigra of the midbrain. The most commonly used treatment strategy is to pharmacologically restore the lost function by the administration of the dopaminergic precursor L-DOPA. Another treatment strategy is to replace the degenerated neurons with immature fetal ventral mesencephalic tissue, or ultimately stem cell-derived tissue. Grafting trials have, however, revealed poor reinnervation capacity of the grafts, leaving much of the striata dopamine-denervated. An additional drawback is the upcoming of dyskinesia (involuntary movements), a phenomenon also observed during L-DOPA treatment of Parkinson's disease patients. Attempts to characterize nerve fiber formation from dopamine neurons have demonstrated that the nerve fibers are formed in two morphologically diverse outgrowth patterns, one early outgrowth seen in the absence of astrocytes and one later appearing outgrowth seen in co-existence with astrocytes.

The overall objective of this thesis has been to study the dopaminergic outgrowth including guidance of nerve fiber formation, and to look into the mechanisms of L-DOPA-induced dyskinesia. The first paper in this thesis characterizes the different outgrowth patterns described above and their relation to different glial cells. The study demonstrated the two different outgrowth patterns to be a general phenomenon, applying not only to dopamine neurons. Attempts of characterization revealed no difference of origin in terms of dopaminergic subpopulations, i.e. A9 or A10, between the outgrowth patterns. Furthermore, the "roller-drum" technique was found optimal for studying the dual outgrowth sequences.

The second and the third paper also utilized the "roller-drum" technique in order to promote both patterns of neuronal fiber formation. The effects of glial cell line-derived neurotrophic factor (GDNF) on the formation of dopamine nerve fibers, was investigated. Cultures prepared from *gdnf* knockout mice revealed that dopaminergic neurons survive and form nerve fiber outgrowth in the absence of GDNF. The dopaminergic nerve fibers exhibited an outgrowth pattern consistent with that previous observed in rat. GDNF was found to exert effect on the glial-associated outgrowth whereas the non-glial-associated was not affected. Astrocytic proliferation was

inhibited using cytosine β-D-arabinofuranoside, resulting in reduced glial-associated outgrowth. The non-glial-associated dopaminergic outgrowth was on the other hand promoted, and was retained over longer time in culture. Furthermore, the non-glial-associated nerve fibers were found to target the fetal frontal cortex. Different developmental stages were shown to promote and affect the outgrowths differently. Taken together, these data indicate and state the importance of astrocytes and growth factors for neuronal nerve fiber formation and guidance. It also stresses the importance of fetal donor age at the time for transplantation.

The fourth and fifth studies focus on L-DOPA dynamics and utilize *in vivo* chronoamperometry. In study four, 6-OHDA dopamine-depleted rats were exposed to chronic L-DOPA treatment and then rated as dyskinetic or non-dyskinetic. The electrochemical recordings demonstrated reduced KCl-evoked release in the intact striatum after chronic L-DOPA treatment. Time for maximal dopamine concentration after L-DOPA administration was found to be shorter in dyskinetic animals than in non-dyskinetic animals. The serotonergic nerve fiber content in the striatum was evaluated and brains from dyskinetic animals were found to exhibit significantly higher nerve fiber density compared to non-dyskinetic animals. Furthermore, the mechanisms behind the conversion of L-DOPA to dopamine in 6-OHDA dopamine-depleted rats were studied. Local administration of L-DOPA in the striatum increased the KCl-evoked dopamine release in the intact striatum. Acute application of L-DOPA resulted sometimes in a rapid conversion to dopamine, probably without vesicle packaging. This type of direct conversion is presumably occurring in non-neuronal tissue. Furthermore, KCl-evoked dopamine releases were present upon local application of L-DOPA in the dopamine-depleted striatum, suggesting that the conversion to dopamine took place elsewhere, than in dopaminergic nerve fibers. In conclusion, these studies state the importance of astrocytes for neuronal nerve fiber formation and elucidate the complexity of L-DOPA conversion in the brain.

ORIGINAL PAPERS

This thesis is based on the following papers, which will be referred to by their Roman numerals:

I. Berglöf E*, af Bjerkén S*, Strömberg I. **Glial influence on nerve fiber formation from rat ventral mesencephalic organotypic tissue cultures.** J. Comp. Neurol. 501:431-442, 2007 *equal contribution

II. af Bjerkén S, Boger HA, Nelson M, Hoffer BJ, Granholm AC, Strömberg I. **Effects of glial cell line-derived neurotrophic factor deletion on ventral mesencephalic organotypic tissue cultures.** Brain Res. 1133:10-19, 2007

III. af Bjerkén S, Marschinke F, Strömberg I. **Inhibition of astrocytes promotes long-distance growing nerve fibers in ventral mesencephalic cultures.** Submitted manuscript

IV. Lundblad M, af Bjerkén S, Cenci MA, Pomerleau F, Gerhardt GA, Strömberg I. **Chronic intermittent L-DOPA treatment induces changes in dopamine release and 5-HT nerve fiber density.** Manuscript

V. af Bjerkén S, Nevalainen N, Lundblad M, Pomerleau F, Gerhardt GA, Strömberg I. **L-DOPA conversion to dopamine in the rat dopamine-depleted striatum.** Manuscript

INTRODUCTION

General history and background

Parkinson's disease is a progressive disorder of the nervous system primarily affecting the motor system of the body. The condition was described as early as 5000 B.C. by Indians practicing the medical system of Ayurveda (Vedas). They referred to the disorder as Kampavata, kampa meaning tremor and vata meaning lack of muscular movement. The Greek physician Galen also described symptoms of the disorder in year 175 A.D, referring to the disease as a "Shaking palsy" (Bendick, 2002). The formal documentation of the disease was, however, first accomplished in 1817 by James Parkinson, a physician in London. In "An Essay on the Shaking Palsy", Parkinson describes the medical history of six persons displaying symptoms of the disease (Parkinson, 2002).

The neuropathology underlying Parkinson's disease was first revealed in 1919 when Trétiakoff found a correlation between the symptoms of the disease and degeneration of dopamine producing neurons in the substantia nigra in the midbrain (Trétiakoff, 1919). Substantia nigra is Latin meaning the black substance, a name referring to the neuromelanin inclusions that are accumulated with age (Mann and Yates, 1983b). Neuromelanin is a non-organic substance thought to develop as a side/waste product of the catecholamine metabolism. In Parkinson's disease, the inclusions disappear along with the dopaminergic neurons as the disease progresses. A pathologic hallmark of Parkinson's disease is the presence of cytoplasmic eosinophilic inclusions termed Lewy bodies in the surviving dopaminergic neurons (Lewy, 1912). The primary component of these inclusions has been found to be the fibrillar form of α-synuclein (reviewed in (Eriksen et al., 2003)).

The neurotransmitter dopamine

Dopamine is an endogenous catecholamine synthesized from the amino acid tyrosine. Tyrosine is converted to dihydroxyphenylalanin (DOPA) by the rate-limiting enzyme tyrosine hydroxylase (TH).

DOPA is then further synthesized to dopamine with the help of the enzyme L- aromatic amino acid decarboxylase (AADC).
Dopamine was first considered as a precursor to adrenaline and noradrenaline, acting as an intermediate in the synthesis. Discoveries in the 1950's did, however, come to change this view when Arvid Carlsson and colleagues demonstrated dopamine to be present in the brain in about similar concentrations as noradrenaline, but with a different distribution (Carlsson et al., 1958). Carlsson also showed that the drug reserpine caused a decrease in dopamine levels resulting in loss of motor control; a loss that could be counteracted by the dopamine precursor 3,4-dihydroxy-L-phenylalanine (L-DOPA) (Carlsson et al., 1957). Reserpine was found to act on the dopamine terminals in the striatum, causing a decrease in dopamine levels by emptying of the terminals (Carlsson et al., 1958). Ehringer and Hornykiewics supported these results, demonstrating reduced dopamine levels in the striatum of patients with Parkinson's disease (Ehringer and Hornykiewicz, 1960). In 2000, Arvid Carlsson was awarded the Nobel Prize for his discoveries, along with his co-laureates Erik Kandell and Paul Greengard.

The regional distribution of dopamine was described in 1964 when Dahlström and Fuxe mapped the dopamine cell groups in the brain (Dahlström and Fuxe, 1964), using the Falck-Hillarp immunohistochemical method (Falck et al., 1962). The dopaminergic nuclei in the ventral mesencephalon (VM) were named A8 (retrorubal area), A9 (substantia nigra; SN), and A10 (ventral tegmental area; VTA).

Clinical features and pathology

The cardinal symptoms of the disease are motor symptoms i.e. muscle rigidity, tremor, hypokinesia and bradykinesia (diminished and slow movements), and postural instability. However, many patients also develop non-motor symptoms as disturbances in mood, cognition, and sensation (reviewed in (Fahn, 2003)). Most of these symptoms are not responsive to dopaminergic replacement therapy; implicating that neurotransmitters other than dopamine are involved in the pathogenesis. In fact, neurodegeneration in Parkinson's disease have been demonstrated in the noradrenergic locus coeruleus (Braak et al., 2003; Mann and Yates, 1983a; Zarow et al., 2003), the serotonergic raphe nuclei (Jellinger and Paulus, 1992), the cholinergic neurons in

the nucleus basalis (Nakano and Hirano, 1984), as well as a number of other nuclei.

Nowadays, the term parkinsonism is commonly used to describe conditions with any combination of at least two of the following features: tremors at rest, bradykinesia, rigidity, loss of postural reflexes, flexed posture, and freezing. There are four categories of parkinsonism - primary parkinsonism, secondary parkinsonism, parkinson-plus syndromes, and heredodegenerative disorders. Primary parkinsonism, or Parkinson's disease, has an idiopathic or genetic etiology, whereas secondary parkinsonism has an environmental etiology. Environmental meaning insults to the brain such as toxins, drugs, trauma, and tumors etc. The third category, the Parkinson-plus syndromes, is characterized by a more extended neurodegeneration as well as poor response to L-DOPA therapy. Heredodegenerative disorders are inherited conditions characterized by neuronal atrophy and dysfunction of neuronal systems. There are three findings that are helpful in distinguishing Parkinson's disease from the other pakinsonisms, in order to set the correct diagnosis, i.e. asymmetrical onset of symptoms, symptomatic response to L-DOPA, and presence of resting tremor (Fahn, 2003).

Etiology

The etiology of primary parkinsonism, i.e. Parkinson's disease, is still unknown. It is has now become clear, however, that there are many different causes of Parkinson's disease, and a number of factors implicated in the pathogenesis. These include oxidative stress, inflammation, mitochondrial dysfunction, excitotoxicity, apoptosis, and proteolytic stress (reviewed in (Olanow, 2007)). An increasing number of genes possibly involved in the pathogenesis have also been demonstrated e.g. α-synuclein, DJ1, Parkin, PTEN-induced kinase 1 (PINK1), ubiquitin carboxyl-terminal esterase L1 (UCHL1), and leucine-rich repeat kinase 2 (LRRK2) (reviewed in (Farrer, 2006)). One of the most recent factors taken under consideration is proteolytic stress. Proteolytic stress arises as a consequence of production of misfolded proteins. Considering the formation of Lewy bodies in Parkinson's disease, it is not unlikely that it is involved in the pathogenesis.

The basal ganglia system

The basal ganglia are a subcortical group of interconnected nuclei consisting of input and output stations. There are four major nuclei of the basal ganglia, the striatum, the subthalamic nucleus (STN), the globus pallidus pars interna (GPi)/pars externa (GPe), and the SN. The substantia nigra is further divided into three subdivisions, the pars compacta (SNc), the pars reticulata (SNr), and the pars lateralis. The striatum and the STN are the major input nuclei, e.g. receiving excitatory glutamatergic input from the cortex and thalamus, dopaminergic input from the SNc, and serotonergic input from the dorsal raphe nucleus. The output nuclei of the basal ganglia include the GPi and the SNr. The striatum is mostly composed of gamma-aminobutyric acid (GABA) medium spiny neurons, but contains also GABAergic and cholinergic interneurons. In addition, the striatum can anatomically and functionally be divided into matrix and striosomes (Graybiel and Ragsdale Jr, 1978). There are two pathways connecting the striatum to the output nuclei, the direct and the indirect (striatopallidal) pathways. The direct pathway projects directly to the GPi and the SNr, whereas the indirect pathway projects to GPi through GPe and the STN. The present basal ganglia model is a development of the Albin-DeLong model (Albin et al., 1989; Alexander et al., 1986; Crossman, 1989; DeLong, 1990), a model stating excitatory input to the striatum from cortex and thalamus, and consequently activation of the striatal projecting neurons. The basic theory of the Albin-DeLong model is still today considered accurate, anatomical investigations have, however, revealed a more complex organization than originally proposed (Figure 1).

The nigrostriatal pathway

The dopaminergic neurons in the SNc project their axons to the striatum creating the nigrostriatal pathway (mesostriatal), part of the basal ganglia. The action of dopamine on striatal neurons depends on the type of dopamine receptors involved. There are two different groups of dopamine receptors, D1-like and D2-like receptors. D1 receptors stimulate adenylate cyclase activity and D2 receptors inhibit adenylate cyclase activity. The receptors are thought to be localized to different striatal output pathways, the direct and the indirect pathway (Gerfen and Wilson, 1996). This is however not fully confirmed since there are implications that D1 and D2 may be co-localized (Lester et

al., 1993; Surmeier et al., 1992), and many striatal neurons have been demonstrated to project simultaneously to the GPe, GPi, and SNr (Parent et al., 2000). The theory is, however, that the normal effects of the dopamine input to the striatum are excitation of the GABAergic medium spiny neurons that project directly to the GPi (direct pathway) and inhibition of the GABAergic medium spiny neurons that project to the GPe (indirect pathway). The direct and indirect pathways together balance the motor control of the basal ganglia. Thus, loss of dopamine in the SNc results in an increase in activity through the indirect pathway and a reduction in activity through the direct pathway, resulting in reduced activity in the output of the basal ganglia. The thalamic activation of the motor cortex is therefore inhibited, for illustration see Figure 1. The reduction in dopaminergic neurons in the SNc, thus, gives the typical manifestations of Parkinson's disease, e.g. hypokinesia, tremor at rest, and rigidity.

Other midbrain dopamine systems are the mesolimbic and the mesocortical which both arise from dopaminergic neurons in VTA. Both systems are involved in emotion-based behavior, such as motivation and award.

Development of the nigrostriatal system

In rat, the cells of the VM are born between embryonic days (E) E11 and E16 and, historically, peak ontogeny have been considered to occur around E13 (Altman and Bayer, 1981; Hanaway et al., 1971; Lauder and Bloom, 1974; Marchand and Poirer, 1983). A recent study suggests, however, the peak ontogeny to occur at E12 (Gates et al., 2006). The midbrain dopamine cells originate at the mesencephalic-diencephalic junction and then migrate to their final location in the VM around E18 (Hanaway et al., 1971; Marchand and Poirer, 1983; Olson and Seiger, 1972; Specht et al., 1981a; Tennyson et al., 1972; Voorn et al., 1988). In rat, immunoreactivity towards TH can be detected at E12.5 (Foster et al., 1988; Specht et al., 1981b) and approximately one day after, at E13-13.5, dopamine can be visualized (Olson and Seiger, 1972; Voorn et al., 1988). Dopaminergic fibers have been demonstrated to reach the striatal anlage at E13.5 (Olson et al., 1972; Specht et al., 1981b). At P14 the ventral mesencephalon has matured, exhibiting adult features (Kalsbeek et al., 1992).

The symptoms of the disease are first seen when the dopamine concentration in the striatum is reduced with 80%, and approximately 60% of the nigral dopamine neurons are lost (Fearnley and Lees,

1991; Marsden, 1990). The loss of dopamine in Parkinson's disease patients is more prominent in the putamen compared to the caudate (Kish et al., 1988; Nyberg et al., 1983), which is a consequence of the more severe loss of dopamine neurons in the ventral tier of the SN (Fearnley and Lees, 1991). Thus, a reduction of the neurons that mainly projects to the putamen (Gibb and Lees, 1991).

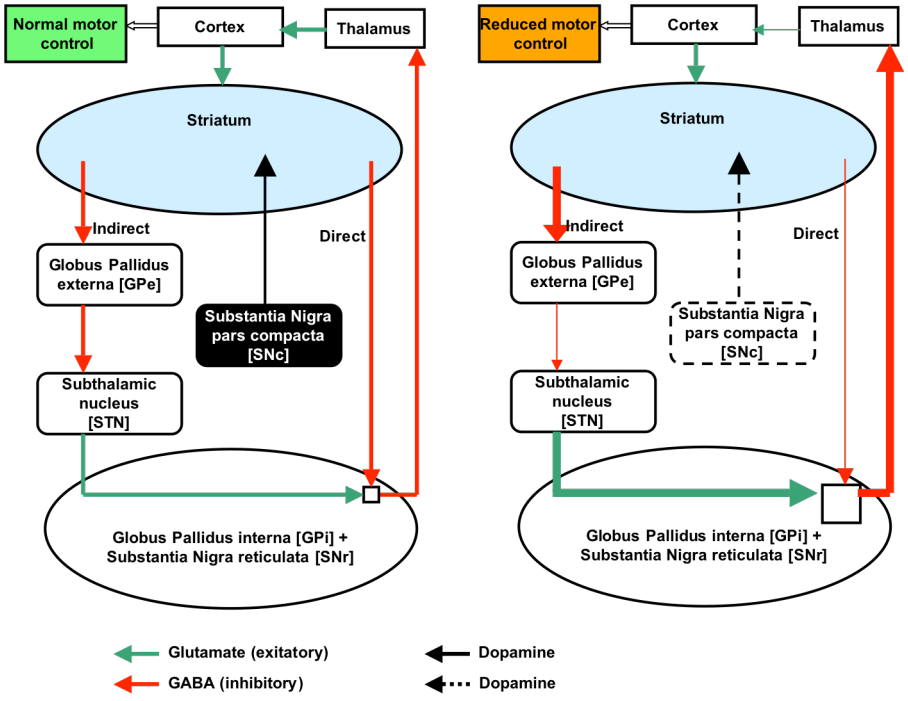

Figure 1. Simplified schemes of the basal ganglia model. The left scheme illustrates the conditions in healthy individuals and the right scheme illustrates the conditions in Parkinson's disease.

Treatment strategies

The discovery of the importance of dopamine in the pathogenesis of Parkinson's disease, along with the effects of L-DOPA seen in reserpine-induced hypokinesia (Carlsson et al., 1957), made researchers focus on L-DOPA as a possible treatment for Parkinson's disease. Unlike dopamine, L-DOPA can pass the blood-brain-barrier further supporting its potential for dopamine replacement therapy. Clinical trials with L-DOPA were undertaken, yet with relatively poor results due to low dosage and side effects such as cardiac arrhythmia and nausea (Barbeau, 1961; Birkmayer and Hornykiewicz, 1961). However, higher dosage along with a stepwise introduction of the drug improved the outcome and it became a useful treatment (Cotzias et al., 1967). This strategy along with peripheral decarboxylase inhibitors further increased the efficacy of the drug, yielding more L-DOPA in the brain (Bartholini and Pletscher, 1968; Dunner et al., 1971; Tissot et al., 1969). L-DOPA therapy in combination with peripheral decarboxylase inhibitors (benzerazid, carbidopa) is still today the most commonly used treatment for Parkinson's disease. Interestingly, the ancient Indians referring to the condition as Kampavata (Vedas) treated the disorder with a tropical legume called Mucuna Pruriens, which seeds have been found to contain high concentrations of L-DOPA (Hussain and Manyam, 1997). Although L-DOPA is effective to treat the symptoms of Parkinson's disease, there are some limitations. After long-term treatment, many patients develop motor fluctuations, such as dyskinesia (involuntary abnormal movements) and decreased drug response (known as "wearing-off") (Granérus, 1978). The loss of drug response can sometimes be counteracted with higher doses of L-DOPA. High doses may, however, result in increased dyskinesia.

Other drugs used to treat the symptoms are dopamine agonists, which act directly on postsynaptic dopamine receptors. The development of dyskinesia and upcoming of the wearing-off effect is less prominent using these drugs. However, side effects as confusion and psychosis are more prone to occur compared to L-DOPA therapy (Rascol et al., 2000). Metabolic inhibitors, such as catechol-O-methyl transferase and monoamine oxidases-B, can also be used to treat the symptoms of Parkinson's disease. The use of a metabolic inhibitor together with L-DOPA can extend its half-life, leaving higher levels in the plasma. Uptake inhibitors can also be used in combination with L-

DOPA, preventing reuptake to the presynaptic terminal, leaving more L-DOPA in the synaptic cleft.

In addition to drug therapy, surgical procedures can be used for treatment of symptoms in Parkinson's disease. Deep brain stimulation is a method were electrical stimulation is utilized to adjust the activity in the basal ganglia. Targets for electrode implantation are, most commonly, either the thalamus, the GP or the STN. Deep brain stimulation was preceded by pallidotomy, a technique, where the GP is destroyed by heat (reviewed in (Narabayashi, 1990)).

A different approach to reduce the symptoms in Parkinson's disease is to replace the lost dopaminergic neurons through transplantation of dopamine producing tissue. Grafting trials with fetal dopaminergic neurons to the striatum of dopamine-depleted rats were performed in the late 1970's (Björklund and Stenevi, 1979; Perlow et al., 1979). The studies were a success, in that they showed a compensatory effect on the motor deficits caused by the dopamine-depletion. Further studies showed long-term survival of the grafts (Freed et al., 1980; Strömberg and Bickford, 1996) as well as an organotypic innervation pattern of the striatum (Björklund et al., 1981; Strömberg et al., 1992). The grafts were functional in that new synaptic connections were formed (Bolam et al., 1987; Clarke et al., 1988; Mahalik et al., 1985; Strömberg et al., 1988), the striatal firing rate was normalized (Fisher et al., 1991; Strömberg et al., 1985; van Horne et al., 1990), and dopamine could be released from the reinnervated striatum (Rose et al., 1985; Strömberg et al., 1988; Zetterström et al., 1986). The first grafting trials in humans were performed using catecholamine-producing cells from the adrenal medulla. Patients received grafts to the caudate (Backlund et al., 1985) or to the putamen (Lindvall et al., 1987), but with disappointing results. The first clinical attempts using human fetal ventral mesencephalon for grafting to parkinsonian patients was published in 1988 (Lindvall et al., 1988; Madrazo et al., 1988). Moreover, postmortem studies of these patients revealed graft survival and reinnervation of the putamen (Kordower et al., 1998). It is now known that transplanted fetal dopamine neurons can survive for over ten years after grafting (Piccini et al., 1999). To date, around 350 patients have received intrastriatal implants of fetal mesencephalic tissue, and a number of open-label trials have reported symptomatic improvement e.g. (Cochen et al., 2003; Hagell et al., 1999; Wenning et al., 1997). The first double-blind study reported less symptomatic improvement

compared to the open-label trials, no improvement was observed in the sham-operated patients (Freed et al., 2001). This study did, however, provide evidence that the improvement is not solely placebo based. A second double-blind trial also demonstrated poor clinical outcome, maybe as a consequence of more severely affected patients taking part in the study (Olanow et al., 2003). Histopathological examination has shown graft survival and reinnervation of the host brain (Kordower et al., 1995). The grafts can also provide functional effects, in that they release dopamine, and become integrated in the neural circuits (Piccini et al., 1999; Piccini et al., 2000). However, the main problem with grafting of fetal dopaminergic neurons is the incapacity of the grafts to sufficiently reinnervate the areas of dopamine depletion. A rat study has shown that the dopaminergic neurons halt in reinnervation shortly after implantation (Barker et al., 1996). Several implant sites are therefore necessary in order to cover the dopamine-depleted striatum. What induces the halt in reinnervation is not known but lack of attractants, such as neurotrophic factors and extracellular matrix molecules, may be a possible cause. Another shortcoming is the development of graft-induced dyskinesias (Freed et al., 2001; Hagell et al., 2002). Furthermore, a major drawback is the poor survival of grafted dopamine neurons, along with ethical concerns using fetal tissue. Therefore, the focus for tissue replacement is today, to a large extent, on the development of stem cells to be used in grafting (for review see e.g. (Correia et al., 2005; Parish and Arenas, 2007)).

Nerve fiber formation

As already mentioned, a way to enhance graft outcome is to improve reinnervation of the host brain. To study factors that influence nerve fiber formation, organotypic tissue cultures can be utilized. Dopaminergic nerve fiber formation has been suggested to occur in two temporally separate waves in organotypic slice cultures of fetal VM, one early and one later occurring wave of nerve fiber outgrowth. The early formed nerve fibers are seen without the presence of glia whereas the later is detected over glial cells (Johansson and Strömberg, 2002). Furthermore, fetal lateral ganglionic eminence (LGE) seems to attract the late occurring wave of dopaminergic nerve fiber outgrowth (Johansson and Strömberg, 2003). The mesencephalic tissue used for transplants and primary cell

cultures contain a mixture of A9 and A10 dopaminergic neurons, as well as A8 dopaminergic neurons (Dahlström and Fuxe, 1964). This might suggest different origins of the observed dopaminergic nerve fiber outgrowths, i.e. that they derive from different dopamine subpopulations.

Neurotrophic factors

Neurotrophic factors are a family of proteins found to support and nourish neurons and nerve fibers. They are responsible for growth and survival during development, but also of importance in the mature brain and nerve system. The first neurotrophic factor found and described was simply named nerve growth factor (Levi-Montalcini and Hamburger, 1953). It was found critical for survival and maintenance of sympathetic and sensory ganglia (Cohen, 1959; Cohen, 1960; Levi-Montalcini and Hamburger, 1953). In 1986, Stanley Cohen and Rita Levi-Montalcini were rewarded the Nobel Prize for their discovery. In the central nervous system (CNS), target neurons synthesize neurotrophic factors acting retrogradely on their afferent neurons (DiStefano et al., 1992; Mufson et al., 1999). Trophic factors can, however, be recruited from other sources as well, e.g. presynaptic neurons (Bartheld, 2004; Conner et al., 1998), and axon-ensheathing glial cells (Creange et al., 1997; Kinameri and Matsuoka, 2003). There are a number of neurotrophic growth factors that may be considered as promoting for ventral mesencephalic dopamine neurons, e.g. glial cell line-derived neurotrophic factor (Lin et al., 1993), brain-derived neurotrophic factor (Hyman et al., 1991), neurturin (Horger et al., 1998), neurotrophin-4 (Hynes et al., 1994), and fibroblast growth factor-2 (Date et al., 1993; Giacobini et al., 1993; Mayer et al., 1993).

Glial cell line-derived neurotrophic factor

In 1993, a novel neurotrophic factor for dopamine neurons was purified. It was found as a secretion product from the rat B49 glial cell line and termed glial cell line-derived neurotrophic factor (GDNF). It was characterized and found to promote the survival of embryonic SN dopamine neurons *in vitro* (Lin et al., 1993). High levels of GDNF mRNA have been detected in developing but not in adult rat striatum (Schaar et al., 1993; Strömberg et al., 1993). GDNF is, however, secreted in low concentrations in the adult striatum and transported retrogradely to the dopaminergic cells in the mesencephalon (Tomac

et al., 1995). This suggests a trophic role for GDNF in the adult brain as well. A few years after the discovery, GDNF was demonstrated to promote survival of dopamine neurons also *in vivo*, both after intracranial administration in the intact rat brain (Hudson et al., 1995) and after administration to parkinsonian rats (Granholm et al., 1997; Strömberg et al., 1993). GDNF gene delivery to the striatum, using viral vectors, has shown to be neuroprotective and promote regeneration in the lesioned nigrostriatal system (Georgievska et al., 2002; Kirik et al., 2000). Moreover, trials with encapsulated GDNF-producing cells to parkinsonian rat striatum revealed protection of both the SN neurons and the striatal fiber innervation (Ahn et al., 2005; Shingo et al., 2002; Yasuhara et al., 2005). A study showed increased density of striatal dopaminergic nerve fibers without changes in SN cell numbers, implicating neuroregenerative properties (Sajadi et al., 2006). GDNF administration into patients with Parkinson's disease has been performed with various outcomes. GDNF injected into the cerebral ventricles did not result in symptomatic improvement (Nutt et al., 2003). A possible explanation is that the GDNF did not diffuse into the brain parenchyma (Kordower et al., 1999), but spread via the cerebrospinal fluid. Therefore, in following studies, the GDNF administration was infused directly into the striatum. Motor improvements in patients chronically infused with GDNF to the putamen (Gill et al., 2003; Slevin et al., 2005), as well as sprouting of dopaminergic fibers (Love et al., 2005) have been reported. In contrast, another study failed to demonstrate motor improvements after GDNF infusion into the putamen (Lang et al., 2006). The study was stopped due to lack of efficacy as well as for safety reasons, since some patients developed antibodies towards GDNF. In addition, a parallel high-dose study in monkeys showed degeneration of cells in the cerebellum.

GDNF signaling is mainly considered to occur through the tyrosine kinase receptor Ret (Durbec et al., 1996) by forming a complex with the glycosylphosphatidylinositol-linked co-receptor 1 (GFRα1) (Buj-Bello et al., 1997). However, studies have also revealed a Ret independent signaling of GDNF (Förander et al., 2001; Poteryaev et al., 1999; Trupp et al., 1999), and that neural cell adhesion molecule (NCAM), together with GFRα1, functions as an alternative signaling receptor for GDNF (Paratcha et al., 2003).

The GDNF knockout mice display deficits in primary sensory, sympathetic, and motor neurons and also fail to develop kidneys,

urethers and most of the enteric nervous system (Moore et al., 1996; Pichel et al., 1996; Sánchez et al., 1996). The GDNF knockout mice die shortly after birth, as a consequence of these deficiencies, limiting research to heterozygous and fetal tissue.

6-OHDA model of Parkinson's disease

The 6-hydroxydopamine (6-OHDA) model (Ungerstedt, 1968) is a common used animal model of Parkinson's disease. 6-OHDA is a hydroxylated analogue of dopamine (Blum et al., 2001), isolated in 1959 (Senoh et al., 1959; Senoh and Witkop, 1959). It was first demonstrated to induce noradrenergic depletion in sympathetic nerves of mice (Porter et al., 1963; Porter et al., 1965), and later found to cause a catecholaminergic specific neurodegeneration in the CNS (Tranzer and Thoenen, 1968). These findings led to the development of an animal model for Parkinson's disease (Ungerstedt, 1968; Ungerstedt and Arbuthnott, 1970). Since 6-OHDA does not cross the blood-brain-barrier, the toxin has to be injected directly into the brain. Preferred injection sites are the SN, the medial forebrain bundle, and the striatum (Perese et al., 1989; Przedborski et al., 1995; Sauer and Oertel, 1994). Depending on the site of injection, different model characteristics are achieved. Following injection into SN or medial forebrain bundle, a rapid degeneration occurs with depleted striatal dopamine levels within 2-3 days (Faull and Laverty, 1969; Hökfelt and Ungerstedt, 1969), whereas an intrastriatal injection causes a slow progressive degeneration (Berger et al., 1991; Przedborski et al., 1995; Sauer and Oertel, 1994). 6-OHDA is most commonly injected unilaterally, causing a hemiparkinsonian model (Perese et al., 1989). Parkinsonian symptoms as bradykinesia and postural abnormalities can be observed already 3 days after lesion. The severity of the degeneration can be assed with drug-induced rotations using amphetamine or apomorphine. Amphetamine acts as an indirect dopamine agonist by increasing the extracellular concentration of striatal dopamine on the intact side, which induces ipsilateral rotational behavior in dopamine-depleted animals (Schwarting and Huston, 1996; Ungerstedt and Arbuthnott, 1970; Ungerstedt, 1971). Apomorphine is a receptor agonist stimulating both D1- and D2-like receptors, with slightly higher affinity for D2-receptors. Systemically administered apomorphine induces rotations contralateral to the

lesion, due to 6-OHDA evoked D2-receptor hypersensitivity in the lesioned striata (Herrera-Marschitz and Ungerstedt, 1984).

Animal model of L-DOPA induced dyskinesia

The rat model of L-DOPA-induced dyskinesia is a development of the 6-OHDA model described above. Chronic administration of low doses of L-DOPA to 6-OHDA hemiparkinsonian rats induces dyskinetic movements contralateral to the lesion (Cenci et al., 1998; Lee et al., 2000). The severity of the dyskinesia is, as in patients, increased over time of treatment, and measured as abnormal involuntary movements (AIMs) (Cenci et al., 1998; Lundblad et al., 2002; Steece-Collier et al., 2003).

AIMS OF THIS THESIS

- To characterize the neuronal and glial cell interactions in fetal ventral mesencephalic slice cultures

- To characterize the two diverse TH-positive nerve fiber formations found in fetal ventral mesencephalic slice cultures, in respect to:

    - glial-association and relation
    - effects of neurotrophic factors, i.e. GDNF
    - fetal tissue age at plating

- To investigate the effects of chronic and acute L-DOPA administration in normal and dopamine-depleted striatum, and in an dyskinetic animal model

MATERIALS AND METHODS

Subjects, animals

Female Spraque-Dawley adult rats (B&K Stockholm, Sweden) or fetuses were used in paper I, III, IV, and V. In paper II GDNF knockout mice generated from the C57BL/6 strain were used (Granholm et al., 1997; Pichel et al., 1996). Heterozygous mice were mated overnight, and the day following mating (day of vaginal plug) was considered day 0.5 of pregnancy. All animals were housed under a 12 h dark/light cycle and were given access to water and pellets *ad libitum*. All experiments were in accordance with internationally excepted guidelines and approved by the local ethics committee.

Dissection of VM, frontal cortex, LGE, and raphe dorsalis

VM, frontal cortex, LGE, and raphe dorsalis (pontine raphe) were dissected from rat or mice fetuses at different developmental stages. In paper I and III, gentle palpation of the abdomen of the pregnant rats were used to decide developmental stage of the fetuses (Olson et al., 1983). Pregnant rats or mice were deeply anesthetized using 4% isofluran (Baxter Medical) before neck dislocation and opening of the abdominal cavity. The uterine horns were isolated and placed in a sterile Petri dish.

All dissections were made using a dissection microscope and performed under sterile conditions. Dulbecco's modified Eagle´s medium (DMEM; Gibco, Grand Island, USA) was used for rinsing and conditioning of the tissue. VM was dissected bilaterally by coronal cuts at the levels of the mesencephalic junction and the mesencephalic flexure. Sagittal cuts were made to disattach the ventral mesencephalic tissue piece (Dunnett and Björklund, 1992; Seiger, 1985), now resembling the wings of a butterfly (connected by the midline). The dissected VM piece comprises besides the A9 (SN) dopamine neurons also the A10 (VTA) as well as the A8 (retrorubal area) neurons (Dahlström and Fuxe, 1964). Fetal frontal cortex was dissected bilaterally and cut into smaller tissue pieces used for culturing. For the LGE dissection, a paramedial cut was made in the

cortex and the cortical tissue piece was folded laterally, exposing the ganglionic eminences. The most lateral part of the striatal anlage was dissected (Pakzaban et al., 1993; Wictorin et al., 1989) and used as one tissue piece for *in oculo* grafting. Fetal pontine raphe was dissected bilaterally between the rhombencephalic isthmus and the pontine flexure. Sagital cuts were made approx. 0.5 mm above the ventral midline on both sides. The dissected tissue was separated at the midline resulting in two pieces used for *in oculo* grafting.

Organotypic primary cultures

VM "roller-drum" cultures

Primary cell cultures were performed using the "roller-drum" technique (Gähwiler et al., 1997; Stoppini et al., 1991). This method ensures a constant flow of medium over the slice culture, minimizing the direct contact with cell debris and other waste products. Cultures were prepared from VM tissue pieces dissected from E12 rat crown-rump length (CRL) = 6-7 mm (paper III), E14 rat CRL = 12-13 mm (paper I and III), E18 rat CRL = 25-28 mm (paper III), or E14 mice CRL = 12 mm (paper II) fetuses. The butterfly shaped tissue pieces were chopped in 300 µm thick coronal sections using a tissue chopper and separated at the midline, each small tissue piece constituting one culture. The GDNF mouse VM tissue, in paper II, was divided into 6 comparable pieces using a scalpel (3 pieces on each side of the midline). All instruments used were sterilized prior to dissection. In paper II, sterilization of the instruments was made in a glass bead sterilizer after each dissected fetus, to prevent DNA contamination. The tissue pieces prepared for culture were plated on 10x24 mm glass coverslips, pretreated with poly-D-lysine (Sigma, Stockholm, Sweden), in a mixture of chicken plasma (Sigma) and thrombin (Sigma). The mixture was left to dry for approximately 20 min before insertion into 15 ml Falcon tubes containing 0.9 ml culture medium. The culture tubes were placed in a "roller drum", turning at speed of 0.5 rpm, in an incubator at 37 ºC and in 5% CO_2. The cultures were supplied with fresh medium every 3-4 day.

VM and fetal frontal cortex "roller-drum" co-cultures

In paper III, E14 rat VM tissue pieces were isolated and co-cultured with pieces of E14 rat frontal cortex. The cultures were prepared as described above and placed adjacent to each other on poly-D-lysine treated coverslips. The cultures were cultivated according to the parameters applying for the single cultures.

VM insert cultures

In paper I, isolated VM tissue pieces were placed and cultivated on membrane insert cultures, pore size 0.4 μM (Millipore, Bedford, MA, USA). The inserts were positioned in wells containing 1.7 ml culture medium and kept at 37 ºC in 5% CO_2. Fresh medium was supplied every 3-4 days.

The organotypic cultures were incubated over different time windows. Paper I: 1, 2, 3, 5, 7, 14, 21, and 28 *days in vitro* (DIV). Paper II: 12 DIV. Paper III: 5, 7, and 14 DIV.

Culture medium

Culture medium was composed of (volume percent) 55% DMEM, 32.5% Hanks' balanced salt solution (Gibco), 10% fetal calf serum (FCS; Gibco), 1.5% glucose, and 1% Hepes (Gibco). The medium was sterile filtered using a 0.22 μm pore size filter (Sterivex; Millipore), and kept in small batches thawed before usage. Additionally antibiotics were added, to a final volume of 1% (10,000 units/ml penicillin, 10,000 μg/ml streptomycin and, 25 μg/ml amphotericin) to the medium at plating, and were thereafter excluded at the first medium change. The medium is well suited for administration of different substances to the tissue. In paper II, recombinant human GDNF (10 ng/ml; Promega, Madison, WI, USA) was added to the medium and in paper III the antimitotic agent cytosine β-D-arabinofuranoside (Ara-C; Sigma) was added in concentrations of 0.5, 1, 2, and 5 μM.

Intracranial (ventricular) grafting (GDNF)

Fetal VM tissue was dissected, as described above, from *gdnf* knockout (n=3), *gdnf* heterozygous (n=1), or wildtype (n=1) E14 fetuses and used for intracranial transplantation. Adult female wildtype mice were deeply anesthetized using 4% isofluran and mounted in a stereotaxic frame for mice. The scalp was cut open, burr holes were made bilaterally over the lateral ventricles (stereotaxic coordinates in mm: AP=±0, ML=±0.8), and the dura mater was pierced using a needle. The dissected VM tissue pieces were divided in the midline rendering two pieces for grafting from each fetus. The tissue was pulled up using a cannula assembled to the stereotaxic frame and lowered into the ventricle (3.5 mm below dural surface) and implanted. The cannula was left in the brain for 1 min before retraction, in order to assure disattachment of the tissue. The scalp was then closed using steel agraffes. The animals were sacrificed 6 weeks postgrafting by intracardial perfusion. All surgical procedures were made under an operating microscope.

Enzyme-linked immunosorbent assay

In paper II, enzyme-linked immunosorbent assay (ELISA) was utilized to determine GDNF protein levels in brain tissue from E14 *gdnf* knockout, *gdnf* heterozygous, or wildtype fetuses as well as in culture medium collected after 3-4 days of incubation (at medium change). The tissue was homogenized with lysis buffer and protease inhibitor, and the GDNF protein levels were determined using a GDNF assay kit (R&D Systems, Abingdon, U.K.). 96-well flat bottom plates were coated with the corresponding capture antibody over night. Duplicate samples of either brains or media were added to the wells and incubated for 2 h at room temperature. Incubation in detection antibody was performed for 2 h followed by incubation with a Streptavidin-HRP antibody. Wash steps removed all unbound conjugates. The plates were incubated with the chromagenic substrate Turbo TMP and an ELISA plate reader was used to monitor the color change. A standard curve using known amounts of GDNF protein was generated to determine sample concentrations.

Genotyping

Polymerase chain reaction (PCR) was performed in paper II and for the GDNF intraventricular grafts in order to genotype the fetal tissue for the presence or absence of the mutant allele.

DNA isolation

Genomic DNA was isolated from fetal tissue not used in culture. The tissue was lysed in 0.5 ml lysis buffer (100 mM Tris pH 8.5, 5mM EDTA pH 8.0, 0.2% SDS, 200 mM NaCl and, 200 mg/ml Proteinase K; Promega) at 56 ºC in a thermomixer (Thermomixer Compact, Eppendorf, Horsholm, Denmark) over night. After lysis, 1 µl/ml Ribonuclease A (RNaseA; Sigma) was added to the homogenates and incubated at 37 ºC for 30 min. Thereafter, 200 µl phenol/chloroform/isoamylalcohol 25:24:1 (Sigma) was added to the samples and the suspensions were centrifuged (14,000 rpm, 5 min). The supernatants were separated from the pellets and mixed with 100 µl chloroform before centrifugation (14,000 rpm, 5min). The supernatants were once more collected and DNA precipitation was performed using 1 ml of cold isopropanol. The DNA was stabilized for 30 min at -20 ºC followed by centrifugation at 4 ºC (14,000 rpm, 5 min). The DNA pellets were washed in 200 µl cold ethanol (70%) and centrifuged (14,000 rpm, 5 min). The purified DNA pellets were dissolved in 200 µl 1 x TE buffer (Promega) at 37 ºC for 2 h.

Polymerase chain reaction

The PCR was performed in a thermal cycler. The DNA was assayed for the presence of the GDNF wildtype or knockout allele in two separate PCR reactions, using primers specific to either the wildtype or the knockout allele. The amplification reaction mixtures, total volume of 20 µl, contained 1.5 µl genomic DNA (or dH_2O for negative controls), 30 µM sense primer: wildtype – 5'-CCA GAG AAT TCC AGA GGG AAA GGT C-3' or knockout – 5'-CGG ACG CGG TTG CGC CTA CCG G-3' (TAG Copenhagen, Copenhagen, Denmark), 30 µM antisense primer, wildtype – 5'-CAG ATA CAT CCA CAC CGT TTA GCG G-3' or knockout – 5'-ACG ACT CGG ACC GCC ATC GGT G-3' (TAG Copenhagen), 250 µM dNTP (Promega), 2 µl 10 x PCR buffer (Promega), 2.5 mM $MgCl_2$, and 2 units of Taq polymerase (Promega). The DNA was amplified for a total of 40 cycles. Each cycle consisted of 1 min denaturation at 92 ºC,

1 min annealing at 56 ºC, and 2 min elongation at 72 ºC. The cycles were preceded by 4 min initial denaturation at 72 ºC.

PCR product analysis

The PCR products were analyzed on a 2% agarose gel (Agarose, LMP preparative grade for small fragments, Promega) using gel electrophoresis. The DNA bands were stained with Ethidium bromide and visualized under UV-light. A 100 bp DNA ladder was used as reference. Amplification of the wildtype allele gave a band of 344 bp, whereas the mutant allele gave a band of 255 bp (Granholm et al., 2000; Pichel et al., 1996).

Dopamine lesions

In paper IV and V, dopamine denervations were performed by unilateral injections of 6-OHDA into the medial forebrain bundle. Rats were anesthetized with 4% isofluran, mounted in a stereotaxic frame, the scalp cut opened and a burr hole was made over the injection site/s at the right hemisphere. 6-OHDA-HCl (Sigma) was dissolved in 0.02% ascorbic acid in 0.9% NaCl and injected into the brain using 10 µl Hamilton syringe, mounted to the stereotaxic instrument. The solution was injected at rate of 1 µl/min and the syringe was left in the brain for 3 min before retraction. After surgery, the scalp was sutured using steel agraffes. All surgical procedures were performed under an operating microscope.

In paper IV, rats weighting approx. 225 g were given two injections of a total of 13.5 µg 6-OHDA-HCl. The injections were performed at the following stereotaxic coordinates in relation to the bregma and the dural surface (in mm): AP = -4.4, ML = 1.2, DV = -7.8, tooth bar = -2.3 (7.5 µg) and AP=-4.0, ML = 0.8, V = -8.0, tooth bar = +3.4 (6 µg). In paper V, young female rats (160 g) were given one injection of a total of 8 µg 6-OHDA-HCl into the medial forebrain bundle at the following coordinates: AP = -4.4, ML = 1.2, V = -7.8, tooth bar = -2.3.

Behavioral testing

Rotational behavior

The efficacy of the 6-OHDA lesions in paper IV and V were assed by drug-induced rotations (Herrera-Marschitz and Ungerstedt, 1984; Ungerstedt and Arbuthnott, 1970).

The first rotational assessment was done approximately 2 weeks after lesion and then repeated on a regular basis. The rats were placed in plastic bowls and strapped into small leashes attached to the recording instrument. Their rotational behavior was then recorded, after drug onset, using a computer program.

In paper IV, i.p. injections of D-amphetamine (Sigma), 2.5 mg/kg in 0.9% NaCl, were used to asses rotations ipsilateral to the lesion. Animals exhibiting > 5 turns per min were selected for further experiments (Winkler et al., 2002). In paper V, rotational behavior was induced by s.c. injections of apomorphine (Apoteksbolaget, Stockholm, Sweden), 0.05 mg/kg in 0.9% NaCl. Animals rotating more than 450 turns contralateral to the lesion, over a time period of 70 min, were selected for further experiments (Heikkila et al., 1981; Herrera-Marschitz and Ungerstedt, 1984; Hudson et al., 1993; Ungerstedt and Arbuthnott, 1970).

Ratings of Abnormal Involuntary Movements (AIMs)

In paper IV, 6-OHDA depleted rats were chronically treated with L-DOPA in order to induce dyskinesia. L-DOPA (Sigma, PURE; 4 mg/kg) was administered i.p. in combination with the peripheral DOPA decarboxylase inhibitor benzerazide-HCl (Sigma; 15 mg/kg) for 14 days. AIMs ratings were done in accordance with the rating scale previously used (Lee et al., 2000; Lundblad et al., 2002) as well as with an amplitude rating scale (Carta et al., 2006). The ratings were performed on days 1, 4, 7, 10 and 14. Ratings were made every 20^{th} min, starting 20 min post L-DOPA injection. The last observation was done 180 min after L-DOPA injection. The animals were ranked either as dyskinetic (global AIM score > 50) or non-dyskinetic. After chronic L-DOPA treatment, 2-3 L-DOPA injections/week were given in order to maintain the dyskinetic behavior. Chronoamperometric measurements were made two days after the last L-DOPA injection in all animals.

Throughout this thesis, the pure L-DOPA form is being consequently used. The pure form in contrast to the more commonly used L-DOPA methyl ester not electrochemically active. Hence, it is better suited for the electrochemical recordings in paper IV and V.

In vivo chronoamperometry

In paper IV and V, *in vivo* electrochemical recordings were performed in rat brains using high-speed chronoamperometric measurement (5 Hz) (Kissinger et al., 1973; Stamford, 1990). The recordings were performed using the FAST-12 system (Quanteon, L.L.C Nicholasville, KY, USA) (Hoffman et al., 1998). Briefly, a carbonfiber electrode is held at a resting potential of 0.0 V vs. an Ag/AgCl reference electrode. The voltage is then instantly stepped to an oxidation voltage of +0.55 V. These square wave pulses are repeated at a rate of 5 Hz, resulting in extracellular oxidation and reduction of oxidizable substances, e.g. dopamine. The chemical reactions induce a rapid change in current recorded by the electrode. The current recorded is directly proportional to analyte concentration (Scatton et al., 1988). Rats were deeply anaesthetized with urethane (1.25-1.5 g/kg bodyweight) i.p. and placed on a heating pad to maintain normal body temperature. Tracheotomy was performed and the animals were allowed to breathe spontaneously. The skull was fixed in a stereotaxic frame, the scalp opened, and the skull and dura mater covering the striatum was bilaterally removed. A single burr hole for the reference electrode was maid on the left hemisphere, approximately 5 mm caudally from the bregma. Carbonfiber electrodes (Quanteon) coated with Nafion (Sigma) were used for the electrochemical recordings. Nafion is a teflon derivate that repells anions, such as ascorbic acid, and enhances the selectivity for cations, such as dopamine (Gerhardt et al., 1984; Nagy et al., 1985). The carbonfiber electrodes were dried at 200 °C for 3 min, swirled in Nafion followed by oven baking at 200 °C for 3 min. The coating procedure was repeated 2-3 times. Electrode calibration was performed to determine sensitivity and linearity. The calibration was assessed in 0.1 M phosphate buffered saline (PBS; pH 7.4) in a beaker using standardized solutions of ascorbic acid (20 mM) and dopamine (2 mM). Electrodes exhibiting high selectivity to dopamine, compared to ascorbic acid, and good linearity were selected for the experiments. The carbonfiber electrodes were assembled with one or two glass

micropipettes using sticky wax. The tip distance between electrode and micropipette was 130-160 µm. The micropipettes were made from glass capillaries (World Precision Instruments, Sarasota, FL, USA) using a pipette puller (PN-30, Narishige, Japan). One micropipette was filled with KCl (120 mM) to evoke potassium-induced dopamine releases, and the other, when used, was filled with L-DOPA (2-10 mM). An Ag/AgCl electrode was prepared in a reference-plating bath, 1 M HCl saturated with NaCl. A silver wire was coated with Cl^- by hooking up the silver wire (future reference electrode) to the anode of a 12 V battery and the cathode to another silver or stainless steel wire. Both wires were then placed in the plating bath for 15-30 min. The Ag/AgCl reference was implanted in the brain, and the electrode/micropipette assembly was then lowered, in the brain, using a microdrive. The micropipettes were connected to a micropressure system allowing pressure ejection of KCl or L-DOPA. Ejections and recordings were performed at different stereotaxic coordinates in the striatum.

Intraocular transplantation

In paper V, the *in oculo* grafting model (Olson et al., 1983) was used to study serotonergic nerve fiber innervation of LGE co-grafts. This is a technique that allows evaluation of the grafts nerve fiber growth, through the transparent cornea. It also provides an isolated *in vivo* milieu, close to the normal authentic, were the graft/s are able to expand without other tissue interference. Furthermore, the blood-brain-barrier of the grafted tissue has been demonstrated to close again approximately 2 weeks after grafting (Granholm et al., 1996).

Grafting of LGE and pontine raphe

LGE and pontine raphe from E14 rat fetuses were implanted under the cornea at different time points. The LGE was implanted and matured for 6 weeks prior to implantation of the pontine raphe. The tissue grafts were placed adjacent to each other on the iris, allowing potential fiber innervation. Briefly, atropine was dropped in the eyes of the graft receiving rats for pupil dilation prior to surgery. The rats were anesthetized with gas anesthesia (4% isofluran) and placed under an operating microscope. A cut was maid in the cornea using a sharp razor and the graft tissue was implanted with a glass pipette.

Chronic L-DOPA treatment

The host rats for the *in oculo* co-grafts were chronically treated with L-DOPA for 21 days, starting at 14 days after pontine raphe implantation. L-DOPA (4 mg/kg) and benserazide-HCl (15 mg/kg) were together dissolved in 0.9% NaCl and injected i.p. once a day.

Tissue preparation and brain sectioning

In paper I, II, and III, organotypic slice cultures were fixed for 1 h in 2% paraformaldhyde in 0.1 M phosphate buffer (pH 7.4). The cultures were, thereafter, rinsed in PBS 3x10 min.

In paper IV, urethane anesthetized rats used for electrochemical recordings, were sacrificed through intracardial perfusion with cold Ca^{2+}-free Tyrode solution followed by 4% paraformaldehyde in 0.1 M phosphate buffer. The brains were dissected and postfixed in 4% paraformaldehyde for 1-2 h at 4 ºC, and then rinsed in 10% sucrose in 0.1 M phosphate buffer (with 0.1% sodium azide) for at least 72 h. The rinsing solution was changed 4-5 times to assure adequate removal of paraformaldehyde from the tissue.

In paper V, brains were dissected out following electrochemical recordings in urethane-anaesthetized rats. The brains were rapidly removed after neck dislocation and immersion fixed in 4% paraformaldehyde for 24 hours at 4 ºC. Rinsing in sucrose-solution was performed as described above.

Intraocular grafts, paper V, were fixed through intracardial perfusion described above. The rats were injected i.p. with an overdose of sodium pentobarbital prior to sacrifice. The grafts were dissected from the eyes together with the irides and postfixed in 4% paraformaldehyde in 0.1 M phosphate buffer. Glucose rinsing was performed according to the same proceedings as above.

The GDNF intraventricular grafts were fixed according to the same proceedings as described for the rat brains in paper IV.

Upon sectioning, the brains were rapidly frozen using gaseous CO_2. Mice (GDNF intraventricular grafting, preliminary data) and rat (paper IV and V) brains were sectioned in 14 µm thick sections using a cryostat. Intraocular grafts were assembled to, and frozen together with, brains for easier sectioning. The frozen sections were mounted on cleaned glass slides pretreated with chrome alun. After sectioning, the tissue was processed for indirect immunohistochemistry or mounted in 90% glycerol in PBS for storage at -20 ºC.

Immunohistochemistry

Cultures

Fixed and carefully rinsed organotypic cultures were incubated with primary antibodies for 48-72 h at 4 ºC in a humid chamber. After primary antibody incubation the cultures were rinsed in PBS for 3x10 min and incubated with secondary antibodies for 1 h at room temperature. The cultures were then again rinsed in PBS for 3x10 min before incubation with 4',6-diamidino-2-phenylindole (DAPI) staining (diluted 1:50) for 10 min at room temperature, for nuclei visualization. Final PBS rinsing for 3x10 min was performed and the cultures mounted on glass slides in 90% glycerol in PBS.

Sections

The slide-mounted sections were thoroughly rinsed in PBS in order to remove glycerol and/or paraformaldehyde. The sections were processed for immunohistochemistry according to the same protocol as for the organotypic cultures, except for DAPI staining which was excluded. Sections of rat SN and the pontine raphe were used for antibody evaluation (not shown).

In paper IV and V, sections of the striata from rats used for electrochemical recordings were immunohistochemically evaluated.

For antibodies and dilutions used see Tables 1 and 2. Antibody dilutions were generally performed in 1% Triton X-100 in PBS for cultures and 0.3% Triton X-100 in PBS for sections. However, the primary antibodies directed against ALDH1 (paper I) and SERT (paper IV and V) were found sensitive to Triton X-100. The primary antibody was therefore diluted in PBS when using these antibodies. Furthermore, these antibody incubations were preceded by a primary blocking step of 10% FCS diluted in 0.3% Triton X-100 in PBS for 1 h at room temperature. After blocking, the sections were quickly rinsed in PBS followed by incubation with primary antibodies.

A second serum block using 5% goat serum was performed before incubation with secondary antibodies in paper III, IV, and V. The goat serum was diluted in PBS and applied for 15 min at room temperature. The blocking solution was gently tipped off after incubation and secondary antibodies were applied.

Table 1. Primary antibodies

Directed against	Type	Dilution	Source	Paper
ALDH1 (aldehyde dehydrogenase-1)	rabbit anti-mouse	1:100	Abcam	I
β-tub (β_{III}-tubulin)	mouse anti-human	1:200	Sigma	I
DARPP-32 (dopamine- and cyclic AMP-regulated phosphoprotein 32 kDa)	rabbit anti-human	1:600	Cell Signaling Tech.	V
GAD65/67 (glutamic acid decarboxylase 65/67)	rabbit anti-human	1:100	Sigma	I
GLAST (glia glutamate transporter)	guinea-pig anti-rat	1:4000	Chemicon	III
Iba1 (ionized calcium binding adapter molecule 1)	rabbit anti-human	1:1000	Wako Chemicals	I
NG2 (NG2 chondroitin sulfate proteoglycan)	rabbit anti-rat	1:200	Chemicon	I
S100	rabbit anti-cow	1:400	Dako Patts	II
SERT (serotonin transporter)	mouse anti-rat	1:400	Chemicon	IV, V
TH (tyrosine hydroxylase)	mouse anti-rat	1:1500	Diasorin Inc.	I, II, III, IV, V
TH	rabbit anti-rat	1:300	Pel Freez, Interassay	I, III
Vimentin	mouse anti-pig	1:200	Sigma	I, III
Vimentin	rabbit anti-calf	1:100	Abcam	III

Tabel 2. Secondary antibodies. Alexa Fluor® conjugates (Molecular Probes Inc., Eugen, OR, USA) were used as secondary antibodies for detection.

Fluorophore	Type	Dilution	Paper
Alexa 594	goat anti-mouse	1:500	I, II, III, IV, V
Alexa 594	goat anti-rabbit	1:500	I, III
Alexa 488	goat anti-guinea pig	1:500	III
Alexa 488	goat anti-mouse	1:200	I, III
Alexa 488	goat anti-rabbit	1:500	I, II, IV, V

Image analysis

Immunohistochemically processed organotypic slice cultures and sections were analyzed using fluorescence microscopy. Photomicrographs were made with a digital camera (Hamamatsu, Solna, Sweden), connected to a computer, and analyzed using the Openlab software (Improvision, Coventry, U.K.). Identical areas were captured at different wavelengths and merged to achieve pictures of double and triple labeling.

Astrocytic migration and fiber outgrowth measurements

Astrocytic migration and nerve fiber outgrowth from fetal VM slice cultures were measured in paper I, II, and III using a scale mounted in one ocular of the microscope. All measurements were performed from the periphery of the tissue slice, defined by the density and depth of DAPI-positive cell nuclei. The astrocytic migration was measured in four perpendicularly placed directions from the periphery of the tissue slice. The nerve fiber outgrowth was measured from the periphery of the tissue slice to the distal end reached by the fibers. For the glial-associated outgrowth, the mean per culture was calculated from 3-4 measurements. The non-glial-associated outgrowth was determined by measuring the distance from the most distal nerve fibers to the periphery of the tissue slice.

Density measurements

In paper II, IV and V, optical density measurements were performed on cultures or sections using the NIH Image software. Images of the same magnitude were captured using a CCD camera (ProgRes C14, Jenoptic, Jena, Germany) and turned binary. The optical density was then measured in a set frame and expressed as gray values.

Cell counting

Cell counts on Iba1-positive cells were performed in paper I. The cells were counted in a set frame in the microscope, in areas over the slice culture. Counting was made over areas dense with TH-positive neurons and over areas with no TH-positive neurons.

Statistics

Statistical analyses were performed using one- or two-way analysis of variance (ANOVA) followed by *post hoc* testing, or using Student's *t*-test. Statistical significance was set at $p<0.05$. All data is expressed as group means ± standard error of the mean.

RESULTS AND DISCUSSION

Characterization of rat fetal VM slice cultures, paper I

In paper I, the TH-positive nerve fiber outgrowth and its relation to astroglia and other glial cells was investigated in rat E14 VM cultures. The organotypic cultures were incubated over a time course of 1, 2, 3, 7, 14, 21, and 28 DIV in order to map the nerve fiber outgrowths and the glial cell migration over time. The occurrence and characteristics of other neuronal nerve fiber formation was evaluated using β-tubulin immunohistochemistry. The results revealed nerve fibers positive for both β-tubulin and TH, as well as nerve fibers only exhibiting β-tubulin-immunoreactivity. This was an important finding revealing the presence of nerve fibers other than TH-positive. Indeed, antibodies directed against GAD65/67 showed the presence of GABA neurons in the VM slice cultures. These findings demonstrate the complexity of the VM cultures, as well as the use of fetal VM for transplantation. The glial content and migration from the cultures were evaluated using antibodies against markers of astrocytes, microglia, and oligodendroglia. The VM tissue slices were cultivated either using the roller-drum technique or on membrane inserts.

Roller-drum cultures

In the organotypic cultures, β-tubulin-positive nerve fibers were observed evenly distributed within the tissue slice and thin fibers were projecting from the slice already at 1 DIV, demonstrating early attachment to the plating surface. Only a few of these nerve fibers displayed immunoreactivity against TH. Hence, TH-immunoreactivity was at this time point mainly found in the tissue slice. At 2 DIV, β-tubulin-positive nerve fiber outgrowth had become more abundant and

the fibers were reaching further from the slice cultures. Moreover, 50% of the cultures displayed, at this time point, TH-positive nerve fiber outgrowth. These TH-positive nerve fibers were less abundant and reached shorter lengths from the tissue slice compared to solely β-tubulin-positive nerve fibers. At 3 DIV, both TH- and β-tubulin-positive nerve fibers increased their length and became more numerous. All nerve fibers found growing outside the tissue slice at 1, 2, and 3 DIV were seen in the absence of glial cells, as revealed by the absence of DAPI-staining. Another characteristic was that nerve fibers extended and projected straight away from the tissue slice without changing direction. At 7 DIV, along with the appearance of glial cell migration, a morphologically different nerve fiber outgrowth pattern was visible. Both TH- and β-tubulin-positive nerve fibers were seen growing onto the migrating vimentin-positive astrocytes**.** This nerve fiber outgrowth formed, in contrast to the initial nerve fiber formation, nerve fiber networks. These mesh-like formations were observed from 14 DIV, and always over vimentin-positive astrocytic monolayer.

The early, in time, occurring nerve fiber outgrowth, found in the absence of glial cell bodies, was still present in cultures at 21 DIV, although not as abundant as at earlier time points. Furthermore, at later time points the initially formed outgrowth often displayed a dotted appearance. This phenomenon was observed in nerve fibers as early as 3 DIV and became more abundant along with the time course. This dotted appearance might be a sign of nerve fiber degeneration or loss of phenotype. In contrast, the nerve fibers growing onto the astrocytic monolayer stayed more persistent over time.

There was a striking difference in outgrowth length from the tissue slice between the two outgrowth patterns. The initial nerve fiber outgrowth, found in the absence of glial cells, reached close to 4 mm from the tissue slice, whereas the later nerve fiber outgrowth, found onto astroglia, reached approximately 1 mm from the tissue slice. Interestingly, intracranial fetal VM grafts are only able to cover a narrow zone surrounding the grafts, before terminated. It appears as if the nerve fiber innervation observed in intracranial grafting to dopamine-depleted striatum is equivalent to the TH-positive nerve fiber outgrowth seen onto the astrocytic monolayer.

To further study these nerve fiber outgrowths, antibodies raised against ALDH1 were used. ALDH1 is an aldehyde dehydrogenase, preferably expressed in A9 compared to A10 neurons (Chung et al., 2005; McCaffery and Drager, 1994). Evaluation of the cultures

revealed nerve fiber outgrowth from the tissue slice occurring in similar patterns as described above. Hence, at 3 DIV nerve fiber outgrowths growing in the absence of glial cells was observed, and later, at 14 DIV, nerve fiber outgrowth was seen onto a layer of vimentin-positive astrocytes. Nerve fibers displaying both TH- and ALDH1-positivity as well as nerve fibers only displaying TH-positivity were observed at both time points, and in both outgrowth patterns. This observation suggests that both nerve fiber patterns may derive from A9 neurons.

The findings of two temporally and morphological different nerve fiber outgrowths in VM slice cultures is supported by earlier results (Johansson and Strömberg, 2002; Johansson and Strömberg, 2003; Takeshima et al., 1994). For simplicity, these different types of nerve fiber formation will, in this thesis, from now on also be referred to as non-glial-associated and glial-associated nerve fibers (Figure 2).

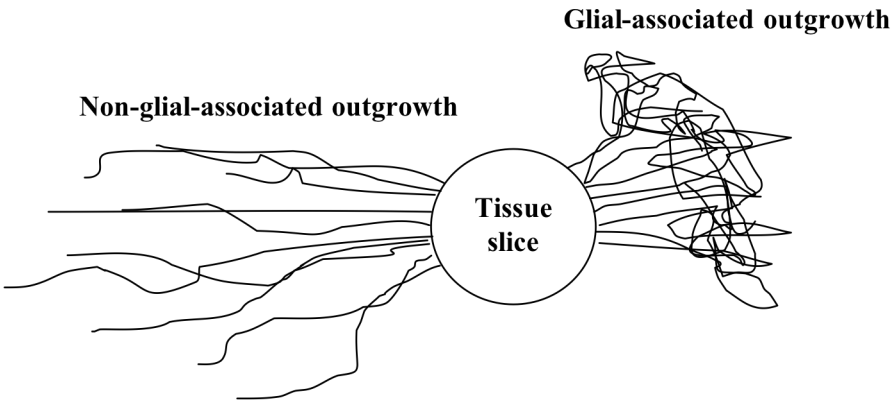

Figure 2. Illustration of the two diverse nerve fiber outgrowths from fetal ventral mesencephalic slice cultures.

Membrane insert cultures

In fetal VM slice cultures incubated on membrane inserts, no TH-positive outgrowth or vimentin-positive astrocytic migration was seen from the tissue slice at 7 DIV. However, at 14 DIV, a few vimentin-positive astrocytes were present outside the tissue slice and TH-positive fibers were observed growing along astrocytic processes. The early occurring TH-positive nerve fibers growing in the absence of astrocytes were not observed.

Different nerve fiber growth patterns depending on culture technique

The membrane insert cultures differed from the roller-drum cultures in that no non-glial-associated nerve fiber outgrowth was observed. Furthermore, the astrocytic migration from the slice was initiated later compared to that observed in roller-drum cultures. Apart from appearing later, no differences in glial-associated nerve fiber formation were found between the culture techniques. The lack of the early, in time, appearing nerve fiber outgrowth in the membrane insert cultures might be speculated to be a consequence of various reasons. Firstly, it might be a question of attachment. In contrast to the roller-drum cultures, the membrane insert cultures were, at plating, not physically attached to the growth surface, instead a self-adherence process was allowed. At 7 and 14 DIV, the tissue cultures had attached to the membrane surface. Since earlier time points were not studied, the time for tissue attachment cannot be determined from this study. It is likely, though, that the non-glial-associated nerve fiber outgrowth was hindered by late attachment of the tissue to the membrane surface. This might also be the reason for late astrocytic migration. Secondly, it might be speculated that the absence of non-glial-associated nerve fibers in the membrane insert cultures is due to lack of growth matrix. The plasma/thrombin clot used for attachment of the roller-drum cultures to the glass surface might function as a matrix, facilitating nerve fiber outgrowth. Similar nerve fiber formations have also been described in a study using gel-embedded nervous tissue (Hernández-Montiel et al., 2008). Furthermore, the plasma/thrombin clot became dissolved in the medium after approximately one week, while non-glial-associated nerve fiber formation was still present and continued to grow. This could suggest that the non-glial-associated nerve fibers are not dependent of supporting matrix or that they need early support in order to project

from the tissue culture. However, solid attachment at plating appears important for the non-glial-associated nerve fibers.

Glial cells in rat fetal VM cultures

In paper I, the presence of glial cells was evaluated over time in E14 VM organotypic roller-drum cultures. Antibodies directed against glia-specific markers as well as DAPI-staining for nuclei visualization were used.

Astrocytes

The astrocytes were visualized using antibodies directed against vimentin. The first astrocytic migration from the tissue slice was seen at 3 DIV, when a monolayer of vimentin-positive cells began to take form. The monolayer displayed different cell morphologies. In close proximity to the tissue slice, thin fibers radiating perpendicularly, from the slice, were observed, whereas more distally, large polygonal cells were seen. Furthermore, vimentin-positive thin fibers were detected in areas distal to the glial migratory border. Interestingly, these distal thin vimentin-positive fibers were often observed over the same areas as the initially formed β-tubulin- and TH-positive nerve growth formations. Hence, although occurring in the absence of glial cell bodies the initial nerve fiber outgrowth pattern are not growing in total absence of glia in fetal VM cultures. The distal vimentin-positive fibers were found to originate and project from large polygonal astrocytes in the periphery of the astrocytic monolayer.

Microglia

Antibodies directed against Iba1, a pan-microglia marker, were used to visualize and evaluate the microglia content of the fetal VM slice cultures. Iba1-positive cells were found at all time points evaluated. The phenotype of the cells differed over time, at 7 DIV the Iba1-positive cells appeared small and round whereas at 14 DIV they had obtained a rougher morphology, with short processes protruding from the cell body. The small rounded cells are believed to move more easily in the tissue compared to more ramified cells. At later time points, 14 and 21 DIV, the Iba1-positive cells were unevenly distributed within the tissue slice. Significantly less Iba1-positive cells were found over areas with TH-positive neuronal cell bodies compared to areas devoid of TH-positive neurons. The reason for this is not known. Nevertheless, microglial cells have been assigned both

good and bad properties (for review see e.g. (Sawada et al., 2006)). Highest amount of Iba1-positive cells were found at 21 DIV to later decline in number at 28 DIV. Moreover, from 14 DIV Iba1-positive cells were found migrating onto the astrocytic monolayer. No relation was, however, found between migrating Iba1-positive cells and nerve fiber outgrowth.

Oligodendrocyte precursors

Oligodendrocyte precursors were visualized in the organotypic slice cultures using antibodies against NG2. Oligodendrocytes may produce growth-inhibiting factors (Cadelli et al., 1992; Kapfhammer et al., 1992), which make them interesting in terms of nerve fiber formation. At 3 and 7 DIV, NG2-positive small rounded cells were found evenly distributed within the tissue slice, and from 7 DIV, NG2-positive cells were also seen migrating away from the tissue slice onto the astrocytic monolayer. Two different morphologies were found among the NG2-positive migrating cells, small round cells and larger more irregular shaped cells. The latter was found at the distal ends of the vimentin-positive monolayer, displaying co-expression with vimentin. No specific relationship was found between NG2-positive cells and TH-positive nerve fiber outgrowth in terms of location. From this study it appears likely that the NG2-positive cells are of no direct importance for TH-positive nerve fiber formation under these conditions.

Effects of GDNF on mice fetal VM slice cultures, paper II

To further study the relation between astrocytes and nerve fiber formations, experiments using tissue from *gdnf* knockout mice were conducted. The promoting effects of GDNF on midbrain dopaminergic neurons, together with the fact that it was originally discovered in a glial cell line (Lin et al., 1993), made it an interesting factor.

Organotypic slice cultures of fetal gdnf gene-deleted tissue

Organotypic slice cultures were prepared from E14 *gdnf* knockout, *gdnf* heterozygous, and wildtype fetuses and incubated for 12 DIV in order to assure astrocytic migration from the tissue slice.

Evaluation of the cultures revealed viable TH-positive neurons in all genotypes as well as TH-positive nerve fiber outgrowth from the tissue slice. No apparent difference in TH-positive cell morphology was observed. Moreover, the TH-positive nerve fiber outgrowths displayed similar patterns and morphologies as observed in paper I, i.e. one early occurring outgrowth seen in the absence of astrocytic cell bodies and one later occurring outgrowth formed onto an astrocytic monolayer. This finding further supports a theory that these two diverse nerve fiber formations would be a general feature. The astrocytes were in this study visualized using antibodies against the calcium-binding protein S100. As a compliment, DAPI-staining was used for detection of additional cell nuclei.

In the cultures, S100-positive astrocytes were seen migrating away from the tissue slice forming an astrocytic monolayer. The S100-positive monolayer reached significantly shorter distances from the tissue slice in *gdnf* knockout cultures compared to *gdnf* heterozygous and wildtype cultures. Interestingly, the addition of exogenous GDNF to the culture medium counteracted this effect, such that the S100-positive astrocytes reached distances of the same magnitude as observed in wildtype cultures. No significant effects of exogenous GDNF were seen on the S100-positive astrocytic migration in *gdnf* heterozygous or wildtype cultures. The glial-associated TH-positive nerve fiber outgrowth reached significantly shorter lengths from the tissue slice in *gdnf* knockout cultures compared to wildtype cultures. The glial-associated TH-positive nerve fiber outgrowth from *gdnf* heterozygous tissue reached lengths between knockout and wildtype. The reduced outgrowth distance seen in the *gdnf* knockout cultures were counteracted by the addition of recombinant GDNF to the culture medium, whereas no significant effects of additional GDNF were found on the distance in *gdnf* heterozygous or wildtype cultures. In addition, exogenous GDNF resulted in increased glial-associated TH-positive nerve fiber density in all genotypes. The non-glial-associated TH-positive outgrowth was, in contrast, neither affected by the *gdnf* deletion nor by the addition of exogenous GDNF. Measurements in wildtype cultures revealed an average length of the non-glial-associated nerve fibers of approximately 3 mm, whereas the average length for the glial-associated nerve fibers was 600 µm from the tissue slice.

GDNF protein levels in culture medium and fetal brain

GDNF protein levels in culture medium and in E14 fetal brains was determined using ELISA. Medium from control cultures showed no detectable levels of GDNF. Thus, the culture medium itself did not contain GDNF, e.g. in the FCS. Culture medium supplemented with additional GDNF revealed no difference in concentration, independent of used for *gdnf* knockout, *gdnf* heterozygous, or wildtype tissue. GDNF was, at medium change, still present in the medium of all genotypes. For the fetal brains, no detectable levels of GDNF were found in the *gdnf* knockout brains and the *gdnf* heterozygous fetal brains showed reduced levels compared to that found in wildtype fetal brains. This experiment demonstrated that no GDNF protein was transferred to the fetuses from the mother, prior to fetal collection or by the control medium.

TH-positive neuronal survival in the absence of GDNF

It can be concluded from paper II that midbrain TH-positive neurons survive the shortcoming of both one and two alleles. This finding is contradictory to a grafting study demonstrating poor TH-positive cell survival in intracranially transplanted fetal VM *gdnf* knockout tissue (Granholm et al., 2000). The grafts in the Granholm et. al. study were implanted in 6-OHDA-depleted striata and left for 8 weeks before evaluation. Interestingly, dopamine-depletion has been demonstrated to upregulate the striatal GDNF levels (Nakajima et al., 2001; Yurek and Fletcher-Turner, 2001), suggesting GDNF availability for the grafts. To further evaluate the survival and viability of TH-positive neurons in *gdnf* knockout tissue, intraventricular grafting was performed. Fetal VM grafts from *gdnf* knockout, *gdnf* heterozygous, and wildtype tissues were transplanted into the lateral ventricles of wildtype mice and left for 6 weeks before tissue fixation and sectioning. Immunohistochemistry revealed viable TH-positive neurons in grafts of all genotypes (Figure 3). Taken together, these findings suggest short-term survival of TH-positive neurons in fetal VM *gdnf* gene deleted tissue.

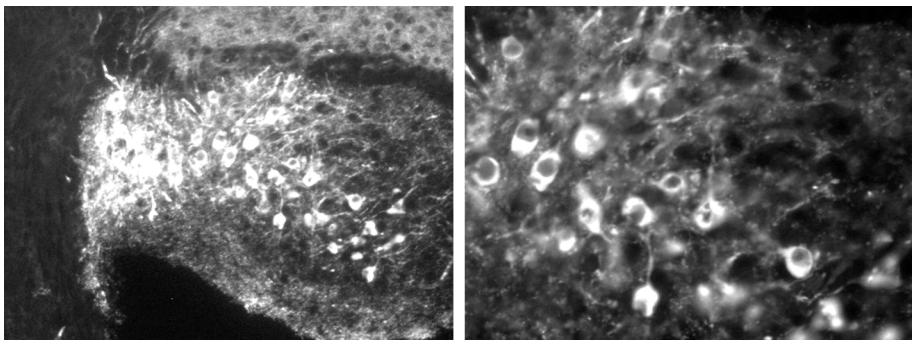

Figure 3. Photomicrographs of intraventricular grafts demonstrating viable TH-positive neurons in *gdnf* gene-deleted fetal tissue.

The effect of GDNF on astrocytes

The decreased length of glial-associated TH-positive outgrowth observed in *gdnf* gene-deleted tissue cultures might be an effect of the reduced astrocytic migration. This is, however, not possible to conclude from this study, since a direct effect of GDNF upon the nerve fibers cannot be excluded. The fact that the non-glial-associated TH-positive outgrowth was not affected by the reduced astrocytic migration favors the idea of decreased glial-associated TH-positive outgrowth length as an indirect effect of reduced astrocytic migration.

The effects of exogenous GDNF on the glial-associated TH-positive nerve fibers in slice cultures might also be due to a direct or indirect effect upon the nerve fibers. Indirect meaning an effect mediated through the astrocytes. A GDNF effect upon the astrocytes is likely to occur since the GDNF receptor GRFα1 have been found on astrocytes under certain conditions (Bresjanac and Antaur, 2000). Since the migration was hampered, it is, though, clear that the astrocytes were affected by the absence of GDNF.

The importance of GDNF for midbrain dopaminergic neurons and nerve fiber formation

The finding that GDNF increases nerve fiber density, in the glial-associated TH-positive nerve fiber formation, suggests that GDNF is important for nerve fiber formation from dopamine neurons. GDNF has been suggested to exert a greater effect on TH-positive neurite formation than on cell survival (Jacobsen et al., 2005), and has been demonstrated to increase the branching points of TH-positive

nerve fibers (Schaller et al., 2005). Moreover, an aging study has demonstrated a reduction in midbrain dopaminergic neurons in aged *gdnf* heterozygous mice compared to wildtype mice (Boger et al., 2006). These results further demonstrate the importance of GDNF for midbrain dopaminergic neurons. There may, though, be discussed if GDNF affects all subpopulations of midbrain dopaminergic neurons. It has been suggested that GDNF affects A10 rather than A9 dopamine neurons (Meyer et al., 1999). GDNF has also been demonstrated to alter the target selectivity for SN dopamine neurons, such that A9 neurons, that normally avoid the cortex, are triggered to innervate the cortex by exogenous GDNF (Jaumotte and Zigmond, 2005).

Inhibition of astroglia in rat fetal VM cultures, paper III

The antimitotic compound Ara-C was utilized to further characterize the non-glial-associated TH-positive nerve fiber outgrowth in organotypic slice cultures. These long-distance growing TH-positive fibers are of interest, since they have been demonstrated to comprise an enormous growth capacity. Roller-drum cultures were prepared from E14 rat fetuses and cultivated over a time course of 5, 7, and 14 DIV, before immunohistochemical processing. The astrocytic cells were visualized using antibodies against vimentin. DAPI staining for nuclei visualization was used as a complement. Ara-C was demonstrated to dose dependently reduce the astrocytic migration from the tissue slice. After evaluating the effect of different Ara-C doses on the slice cultures, a concentration of 1 μM Ara-C was selected for the further study. This dose resulted in a clear effect on vimentin-positive migration, without any apparent effect on the TH-positive cell viability. These results are somewhat contradictory to a previous study demonstrating no astrocytic survival using a dose of 0.05 μM (Johansson and Strömberg, 2002). The Johansson and Strömberg study used, however, antibodies against S100 and glial fibrillary acidic protein for glial cell detection, and not vimentin, as in this study. Since vimentin is an early astrocytic marker these findings cannot be directly compared with previous results.

In the cultures, the two temporally diverse TH-positive outgrowths displaying the same morphology and characteristics as described in papers I and II were found, i.e. non-glial-associated and glial-associated outgrowths. The Ara-C inhibitory effect on the

astrocytic migration was observed at 7 and 14 DIV. The TH-positive non-glial-associated nerve fibers were radiating from the tissue slice at 5 DIV with no vimentin-positive cells, or any other cells present. The Ara-C treatment did not affect the length of the TH-positive non-glial-associated fibers. However, it did increase its persistence, in that a higher percentage of Ara-C treated cultures compared to control cultures displayed non-glial-associated TH-positive fibers both at early and late time points. This might be an indirect effect of the reduced astrocytic migration, since the results in paper I and II suggest complex dynamics between the existence of the two diverse TH-positive outgrowth patterns and the astroglia.

The glial-associated TH-positive nerve fiber outgrowth was observed in cultures from 5 DIV but became more abundant at later time points. The Ara-C treatment was found to significantly reduce the glial-associated TH-positive fiber outgrowth from the tissue slice at 14 DIV. No reduction in outgrowth was observed between control and Ara-C treated cultures at earlier time points. This late inhibitory effect is probably a consequence of the Ara-C-induced delayed onset of astrocytic migration, seen first at 7 DIV.

Importance of fetal age upon grafting

In paper III, fetal VM roller-drum cultures were prepared from E12, E14, and E18 rat fetuses in order to investigate the influence of tissue age at plating on the two diverse TH-positive outgrowth patterns. The vimentin-positive astrocytes were found to migrate for different lengths from the tissue slice depending on fetal age at plating. The vimentin-positive cells in the E12 cultures reached significantly shorter distances from the tissue slice compared to both E14 and E18 derived cultures, and the vimentin-positive astrocytes in the E14 cultures reached significantly shorter distances compared to E18 cultures, at 7 DIV. Differences in TH-positive nerve fiber outgrowth were also found between the fetal stages. At 7 DIV, the E12 cultures demonstrated a robust non-glial-associated TH-positive outgrowth whereas the glial-associated TH-positive outgrowth was barely detected. The TH-positive neurons in the E12 cultures were small in size and appeared to be more numerous compared to those found in E14 and E18 cultures. The TH-positive outgrowths in E14 cultures were found exhibiting the same characteristics as described for the control cultures above. No nerve fiber outgrowth was found in the E18 cultures. TH- as well as β-tubulin-positive neurons had

instead migrated away from the tissue slice. The reason for this is not clear. Dopamine neurons have migrated to their final position at the stage of E18 (Shults et al., 1990) and should already be positioned in our E18-derived cultures. One possible explanation is an alteration in growth promoting or inhibiting signals. This study demonstrates the importance of fetal age for optimal grafting results. The recent reconsideration of the midbrain dopamine cell ontogeny, with a peak at E12 (Gates et al., 2006) and higher survival rate of E12-compared to E14-derived grafts (Torres et al., 2007) suggests E12 VM as a better choice for grafting than the commonly used standards of E14. For experimental trials, it is, however, not only the age of the VM tissue that is of importance, the age of the striatum has been demonstrated of equal importance (Strömberg et al., 1997).

Radial glia in VM cultures

Thin vimentin-positive fibers with no cell bodies present, also described in paper I, were often found extruding and radiating from peripheral vimentin-positive cells. These processes were most prominent in E12 cultures and were often found in the same areas as non-glial-associated TH-positive nerve fibers. Moreover, these thin fibers demonstrated co-existence with GLAST, here used as a marker of radial glia (Shibata et al., 1997). The function of radial glia has recently been reconsidered, from being a scaffold for neuronal migration (Hidalgo et al., 1995; Hidalgo and Booth, 2000) to represent a population of neuronal progenitors (Heins et al., 2002; Malatesta et al., 2003; Merkle et al., 2004; Spassky et al., 2005). The thin non-neuronal vimentin/GLAST-positive fibers might therefore be destined for a fate other than astroglial.

Fetal VM and cortex co-cultures

Rat E14 VM and cortex were co-cultured using the roller-drum technique. This was performed in order to study the two diverse TH-positive nerve fiber formations in the presence of a possible growth target. The non-glial-associated TH-positive nerve fibers were seen to grow into the cortex. The glial-associated TH-positive nerve fibers appeared, on the other hand, not affected by the cortical tissue. Thus, this experiment suggests cortex as a possible target for the non-glial-associated TH-positive nerve fibers.

Dopaminergic subpopulations in fetal VM cultures

The fetal ventral mesencephalic slice cultures in papers I, II, and III consisted of a mixture of dopaminergic neurons (Dahlström and Fuxe, 1964). The A9 cell group (SN neurons) confines its outgrowth to the caudate and the putamen (dorsal striatum) (Huang, 1990), whereas the A10 cell group (VTA neurons) innervate the nucleus accumbens (ventral striatum) and the cortex (Chronister et al., 1980; Kalsbeek et al., 1988). There are proposed markers for the different dopaminergic subpopulations, e.g. calbindin for A10 neurons (Gerfen et al., 1985; Gerfen et al., 1987; German and Liang, 1993), the inward-rectifying potassium channel Girk2 (Schein et al., 1998) and ALDH1 (Chung et al., 2005; McCaffery and Drager, 1994) for A9 dopamine neurons. The two morphologically different TH-positive nerve fiber formations found in organotypic slice cultures in papers I, II, and III might derive from different dopaminergic subpopulations. The cortex and VM co-cultures in paper III supports this idea, demonstrating the cortex as a possible target for the non-glial-associated TH-positive nerve fibers. Moreover, a previous co-culture study revealed LGE as a possible target for the glial-associated TH-positive nerve fibers, whereas the non-glial-associated nerve fibers were seen avoiding it (Johansson and Strömberg, 2003). The non-glial-associated outgrowth would then possibly be A10-derived, and the glial-associated growth would, possibly, be A9-derived. Furthermore, an intraventricular grafting study has demonstrated, using retrograde tracing, a subpopulation of TH-positive neurons that do not project and grow into the striatum. These neuronal cell bodies were calbindin-positive, suggesting them to be A10-derived (Törnqvist et al., 2001). Taken together, these findings favor the idea that the diverse nerve fiber formations originate from different midbrain dopaminergic populations. There are, however, contradictory findings to the subpopulation theory. ALDH1 immunoreactivity was found in both types of TH-positive outgrowth, suggesting both outgrowth patterns to be A9-derived. If this is the case, there are still possibilities of subpopulatory origin of the two diverse TH-positive nerve fiber outgrowths, i.e. they could be derived from either the ventral or the dorsal tier of the SN.

Grafting of fetal midbrain dopamine neurons

The results in paper I-III are of importance for the development of functional grafts for patients with Parkinson's disease. As

mentioned in the introduction, the main problem with grafting of fetal dopaminergic neurons is the incapacity of the grafts to sufficiently innervate the areas of dopamine depletion. More knowledge about the midbrain dopaminergic neurons and their fibers will increase our ability to guide and direct the graft-derived nerve fiber outgrowth. However, another drawback with midbrain dopaminergic transplantation is the upcoming of graft-induced dyskinesias in some of the grafted patients (Freed et al., 2001; Hagell et al., 2002; Olanow et al., 2003). This side effect of grafting therapy has been suggested to be due to the uneven distribution of dopamine nerve fibers, caused by multiple implantation sites, creating so called dopamine "hot spots" (Maries et al., 2006). This further strengthens the needs for control of nerve fiber outgrowth. Dyskinesia is also often developed after chronic L-DOPA treatment in patients with Parkinson's disease. Therefore, in paper IV and V, *in vivo* electrochemistry were utilized to investigate the effects of L-DOPA in the striatum of 6-OHDA depleted rats, with or without dyskinesia.

Effects of L-DOPA in a rat model of dyskinesia, paper IV

In paper IV, the effects of L-DOPA were investigated in a rat model of dyskinesia. 6-OHDA lesioned animals were chronically treated with L-DOPA over 21 days in order to induce dyskinesia (Cenci et al., 1998; Lundblad et al., 2002). Before initiation of L-DOPA treatment, the turning behavior of the animals was tested using amphetamine-induced rotations.

AIMs ratings

The L-DOPA-induced dyskinesia was monitored using the rat AIM rating scale (Carta et al., 2006; Cenci et al., 1998; Lee et al., 2000; Lundblad et al., 2002). Dyskinetic behavior was observed already during the first week of chronic L-DOPA treatment, with a majority of the animals developing severe AIMs. The animals were divided into dyskinetic or non-dyskinetic based on the results of the AIMs rating.

In vivo chronoamperometry, electrochemical recordings

Measurements of extracellular dopamine upon KCl-stimulation were monitored in drug naïve normal and 6-OHDA lesioned control rats and in 6-OHDA lesioned animals chronically treated with L-DOPA, with or without L-DOPA-induced dyskinetic behavior. The measurements were performed pre- and post acute systemic L-DOPA administration, in both hemispheres of the animals. In order to study both release in resting state and release in a challenged system two KCl ejections were made at each striatal-recording site, i.e. a 1st and a 2nd ejection/stimulation. The 2nd ejection was performed only 120 seconds after the 1st ejection hindering full recovery of the system.

Overall findings

The amplitude of potassium-evoked dopamine release was, as expected, very low in the lesioned striata, measuring approximately 5% of that observed in the control striata. Changes in the uptake and release dynamics were also found. Both the T_{rise}, time to reach peak amplitude, and the T_{50}, time measured from maximal amplitude until the concentration had reached 50% of maximal concentration, were significantly increased in the dopamine-lesioned striata compared to normal/control. Moreover, in the lesioned striatum, the uptake rate, calculated as the slope constant multiplied with the peak amplitude, was reduced by an average of 95% compared to the intact side. Hence, released dopamine stayed longer in the extracellular space in dopamine-depleted striata compared to normal/control striata, leading to better availability of dopamine. It is, thus, possible that the reduced reuptake is due to a compensatory mechanism counteracting the effects of the decreased dopamine release. If so, this could explain why behavioral effects are first observed when 70-80% of the dopaminergic neurons are lost (Hudson et al., 1993). Another possible explanation would be reduced uptake due to decreased availability of the dopamine transporter in lesioned striatum (Friedemann and Gerhardt, 1992; van Horne et al., 1992).

Effects of chronic L-DOPA treatment

The peak amplitude of the 1st KCl-stimulation before acute L-DOPA administration was significantly reduced with approximately 60% in the intact side of both dyskinetic animals and non-dyskinetic animals, compared to normal and the intact hemisphere of unilaterally dopamine-depleted drug naïve animals. For the 2nd KCl-stimulation,

the same tendency was observed. Hence, chronic L-DOPA treatment reduced the amplitude of KCl-evoked dopamine release in intact sides of the striatum. Furthermore, no relation to chronic L-DOPA treatment and differences in uptake and release dynamics were found. For lesioned striatum, no differences in amplitudes or release kinetics were found in chronic L-DOPA treated dyskinetic or non-dyskinetic animals compared to L-DOPA naïve animals. The finding that chronic L-DOPA treatment reduced the peak amplitude of KCl-evoked dopamine release in the intact striatum is contradictory to a microdialysis study showing increased striatal dopamine levels in the intact side after L-DOPA administration (Miller and Abercrombie, 1999). However, high extracellular levels of dopamine would theoretically affect the dopamine autoreceptor and a reduced release should be seen.

Effects of acute L-DOPA administration

Acute L-DOPA administration significantly reduced the peak amplitude of measured dopamine after the 1st KCl-stimulation in the intact side of all animals. Trends towards reduced levels were also observed after the 2nd KCl-stimulation in all groups. In the lesioned sides, no significant differences in KCl-evoked peak amplitudes were observed after acute L-DOPA administration compared to before. T_{rise} after acute L-DOPA was longer in the dopamine-denervated hemisphere of non-dyskinetic and lesion controls than in dyskinetic animals, displaying a T_{rise} comparable to normal animals, after the 2nd KCl-evoked release. Thus, it appears as the dyskinetic animals reach maximal concentrations, following KCl-stimulation, faster compared to the non-dyskinetic animals.

TH-positive nerve fiber density

TH-immunohistochemistry revealed few or no TH-positive nerve fibers in the 6-OHDA-lesioned striata, confirming the amphetamine-induced rotational behavior. Measurements revealed a reduction in TH-positive nerve fiber density of more than 98% in the dopamine-depleted hemisphere compared to normal or intact hemispheres. No differences were found between any of the lesioned animals.

SERT-positive nerve fiber density

For 5-HT nerve fiber detection, antibodies against SERT were used. The rational of using SERT, as a marker for serotonergic neurons, is the rapid post mortem diffusion of 5-HT in the brain. Density measurements revealed a significant decrease in dopamine-depleted striatum of lesioned control and non-dyskinetic animals. In contrast, the SERT-positive nerve fiber density in dyskinetic animals was not different from that found in normal animals. This demonstrates that the two-injection-site 6-OHDA-lesion model used in this study, besides dopaminergic denervation, also causes a denervating effect on the striatal serotonergic nerve fiber content. It might be argued that the SERT-positive nerve fibers were spared or not affected by the 6-OHDA lesions in dyskinetic animals. This is, however, not likely considering the reduced nerve fiber levels in lesioned control animals. It seems, thus, as the chronic L-DOPA treatment have induced 5-HT sprouting and nerve fiber regeneration in the dyskinetic animals, restoring the levels to normal. Indeed, serotonergic hyperinnervation of the striatum have been found after neonatal 6-OHDA lesioning of the nigrostriatal dopaminergic system (Luthman et al., 1987). The putative nerve fiber regeneration in some animals (i.e. the dyskinetic) and not in others (i.e. the non-dyskinetic) is hard to conceive. It appears, though, possible that the dyskinetic animals might have had more 5-HT nerve fibers spared after the 6-OHDA lesions, facilitating presumable sprouting. It may further be speculated that the SERT-positive nerve fiber density, comparable to normal, in the dyskinetic animals in combination with the loss of TH-positive nerve fibers might lead to dyskinesia. Moreover, serotonergic neurons contain AADC, which is needed for the conversion of L-DOPA to dopamine (Hökfelt et al., 1973; Lovenberg et al., 1962). It is, thus, possible that L-DOPA is uptaken into serotonergic nerve terminals and then converted to dopamine. The converted dopamine would then possibly be released together with 5-HT. Indeed, using immunohistochemistry, it has been demonstrated that dopamine is localized in cell bodies of the raphe nuclei as well as in striatal serotonergic nerve fibers after L-DOPA administration (Arai et al., 1995). In addition, the striatal dopamine levels after L-DOPA in animals with combined dopaminergic and serotonergic denervations, are decreased compared to solely dopamine-denervated animals (Tanaka et al., 1999). Together, these results demonstrate that serotonergic nerve terminals in the striatum can convert exogenous

administered L-DOPA into dopamine, and may be part in the upcoming of dyskinesia. Furthermore, serotonergic hyperinnervation has been shown to aggravate dyskinesia (Carlsson et al., 2007). In the present study, there was a difference in serotonergic nerve fiber density, seen by SERT immunohistochemistry, between the groups. However, no differences in peak amplitude of released dopamine were detected, suggesting that other nerve fibers, apart from dopaminergic and serotonergic, or tissues could be involved in the conversion of L-DOPA to dopamine.

The conversion of L-DOPA to dopamine in dopamine-depleted striatum, paper V

In paper V, the conversion of L-DOPA to dopamine was studied in 6-OHDA-lesioned rats. Potassium-evoked releases of dopamine were studied before and after local administration of L-DOPA into the striatum of normal control rats, intact hemisphere of 6-OHDA-lesioned rats, and in the lesioned hemisphere of 6-OHDA-depleted rats.

Different L-DOPA phenomena

Pure L-DOPA ejected into the striatum gave sometimes rise to immediate signals of dopamine. This occurred both in normal and 6-OHDA-depleted striata. When detected, either a signal with a rapid onset or a signal with slow rise occurring over long time was found.
It was, independent on response, possible to induce KCl-evoked releases after the L-DOPA ejections.

Effects of local striatal ejections of L-DOPA

Normal animals

Local administration of L-DOPA into normal striatum significantly increased KCl-evoked peak amplitudes. No differences regarding recording sites were seen. Moreover, the peak amplitudes did not differ, regardless of a rapid response of dopamine. No differences in uptake and release dynamics were found. This finding is contradictory to paper IV where L-DOPA was demonstrated to decrease the peak amplitudes of potassium-evoked dopamine releases in intact striata of dyskinetic and non-dyskinetic animals. However, the results are not directly comparable considering that the present

study was accomplished using locally applied L-DOPA, whereas systemically L-DOPA administration was used in paper IV.

Intact hemispheres of 6-OHDA lesioned animals

In the intact hemisphere of 6-OHDA depleted rats, significantly higher peak amplitudes were detected after L-DOPA administration compared to the peak amplitudes observed after L-DOPA ejection in normal rats. No significant differences in amplitudes were observed between normal and intact hemisphere of lesioned animals before L-DOPA administration. The measurements did neither reveal any differences in uptake nor release dynamics before or after local L-DOPA ejection. The intact side of 6-OHDA lesioned animals appears to upregulate its capacity for dopamine production.

Lesioned striatum

KCl-evoked releases of dopamine were proven possible after local L-DOPA administration in 6-OHDA lesioned striatum. Before L-DOPA ejection, no or small amplitudes were seen after KCl-stimulation. Significant increases in peak amplitude upon KCl-stimulation were observed after L-DOPA ejection compared to before giving L-DOPA. However, to achieve a dopamine signal upon L-DOPA loading, higher dose of L-DOPA than given in control side was needed. No differences related to striatal coordinates were found, as well as no differences in uptake and release dynamics before and after L-DOPA loading.

Evaluation of the SERT-positive nerve fiber density

The SERT-positive nerve fiber density was evaluated in the brains from normal and unilaterally 6-OHDA lesioned rats. The measurements revealed no differences in SERT-positive nerve fiber density between the intact or lesioned sides or in normals. However, differences in SERT-positive nerve fiber density along the dorsoventral axis were found. Significantly higher nerve fiber density was found at -5.5 mm compared to -3.5 mm from the dural surface. The unilateral 6-OHDA lesions were in this study performed using single SN injections of the toxin. In contrast to the reduced density of SERT-positive nerve fibers of the lesioned control striata seen in paper IV, this single-site administration of 6-OHDA appears not to damage the serotonergic striatal nerve fibers. This suggests that these two different methods of 6-OHDA administration create completely

different conditions. The method of choice must, therefore, be considered carefully before experiments are conducted.

L-DOPA effects on SERT-positive nerve fibers

LGE and pontine raphe co-grafts were accomplished using the *in oculo* model. Due to poor attachment between the co-grafts no conclusions regarding possible SERT-positive nerve fiber innervation into the LGE could be drawn. However, a slight tendency towards increased SERT-positive nerve fiber innervation within the pontine raphe itself was observed after L-DOPA treatment.

L-DOPA conversion to dopamine

It can be concluded from this study that L-DOPA can be converted to dopamine in dopamine-depleted striatum after local L-DOPA administration. However, high doses of L-DOPA have to be loaded into the striatum before KCl-evoked release is possible. L-DOPA is probably accumulated in neurons, converted to dopamine, and stored in synaptic vesicles. It is possible for this to take place in serotonergic nerve fibers, considering the presence of AADC and the vesicular monoamine transporter 2 (VMAT) (Arai et al., 1995; Nirenberg et al., 1995; Peter et al., 1995). In paper IV, no relation between serotonergic nerve fiber density and peak amplitude after acute systemic L-DOPA administration was found. A previous study does, however, demonstrate a relation between peak amplitude and nerve fiber density (Strömberg et al., 1991). Furthermore, no differences in peak amplitudes in dorsoventral direction from the dural surface were found. If the density of serotonergic nerve fibers were of importance, increased peak amplitudes would have been expected at deeper levels in the striatum, since serotonergic nerve fiber density increased in the in dorsoventral direction. It is therefore likely that nerve fibers other, than the serotonergic, are involved in the conversion of L-DOPA to dopamine as well. The reason for a detectable dopamine signal immediately or shortly after L-DOPA ejection is not clear. It appears, however, as the L-DOPA is instantly converted and released as dopamine, an event that is unlikely to occur in nerve fibers, considering the time for vesicular packing of the dopamine. The instant conversion of L-DOPA to dopamine is therefore more likely to take place in non-neuronal tissue (Sarre et al., 1994). Indeed, conversion of L-DOPA to dopamine has for example been found possible in blood capillaries (Melamed et al., 1980). A

cytosolic release of dopamine, without vesicular packaging, might also be conceivable. The peak amplitude of those rapid signals indicates that this source of L-DOPA conversion might have great impact on dopamine levels in dopamine-depleted striatum.

CONCLUDING REMARKS

Dopaminergic nerve fiber formation in organotypic slice cultures

In paper I, a possible relation between astrocytes and nerve fiber formation in fetal VM cultures was suggested, with one initially formed nerve fiber outgrowth observed in the absence of astrocytes and one secondly formed nerve fiber outgrowth observed in the presence of astrocytes. Furthermore, antibodies directed against the pan-neuronal marker β-tubulin displayed nerve fiber outgrowths with similar characteristics as that seen for the TH-positive outgrowths, with two temporally and morphologically different nerve fiber formations. This phenomenon appears not to be exclusive for TH-positive nerve fiber formation and could be considered as a general mechanism. The theory of a general nerve growth mechanism was supported by the results in paper II, demonstrating equal nerve fiber formations in mice, as well as by the results in paper III.

There was a striking difference in outgrowth length between the two outgrowth patterns. The non-glial-associated nerve fibers, reached close to 4 mm from the tissue slice, whereas the glial-associated nerve fibers reached approximately 1 mm from the tissue slice. The extreme length of the non-glial-associated outgrowth demonstrated an enormous growth capacity of midbrain dopaminergic neurons. In contrast, intracranially grafted fetal midbrain dopaminergic neurons are only able to innervate a narrow zone surrounding the graft. The reason for poor innervation of the host brain could be due to lack of signals and attractants. However, the long-distance growing non-glial-associated fibers might not be destined for striatal innervation, since these fibers were seen growing into the cortex.

Importance of GDNF for dopaminergic nerve fiber formation

Fetal midbrain dopaminergic neurons survived in the absence of GDNF. This was demonstrated both by organotypic culturing and intraventricular grafting of fetal *gdnf* knockout tissue. Furthermore, in organotypic cultures, the gene-deletion reduced both the astrocytic

migration and the non-glial-associated dopaminergic nerve fiber outgrowth from the tissue slice. Both effects were counteracted by exogenous GDNF, which also increased the density of the dopaminergic outgrowths in all genotypes. GDNF did not affect the non-glial-associated nerve fibers. Taken together, GDNF appears of importance for dopaminergic nerve fiber formation and especially in terms of nerve fiber density.

Importance of astrocytes for dopaminergic nerve fiber formation

A close relation between astrocytic migration and dopaminergic nerve fiber outgrowth was found in papers I and II. The importance of astrocytes for dopaminergic nerve fiber outgrowth was further stated in paper III, where the presence or absence of astrocytes was found to affect the two diverse nerve fiber formations differently. Inhibition of astrocytic migration reduced the glial-associated outgrowth, whereas the non-glial-associated outgrowth was promoted, remaining longer in culture.

Thus, it can from paper I-III be concluded that the two diverse dopaminergic nerve fiber formations are dependent on astrocytes, i.e. the presence or absence of them. Furthermore, the characterization of fetal midbrain dopaminergic neurons and nerve fiber formation are of importance for future grafting trails. More knowledge about the nerve fibers and their growth characteristics is necessary to improve the success rate of future grafting therapy, regardless using fetal- or stem cell-derived tissue.

Chronic and acute L-DOPA effects

Chronic L-DOPA treatment reduced the potassium-evoked dopamine release in intact striatum in paper IV, an effect further strengthen by acute systemic administration of L-DOPA. This is in contrast to the finding in paper V, where local L-DOPA administration in the striatum resulted in increased potassium-evoked dopamine release in intact striatum. Neither chronic nor acute L-DOPA affected the amplitude of potassium-evoked dopamine release in the denervated striata in dyskinetic or non-dyskinetic animals. Furthermore, a relation between serotonergic nerve fibers and

dyskinesia was found, in that the dyskinetic animals displayed significantly higher serotonergic nerve fiber density compared to non-dyskinetic animals.

In study V, it was demonstrated that L-DOPA can be converted to dopamine in dopamine-depleted striatum, and then be released upon potassium stimulation. The serotonergic nerve fiber density did not affect the amplitude of the released dopamine, which suggests the conversion of L-DOPA to dopamine to take place not only in the serotonergic nerve fibers in dopamine-depleted striata. Interestingly, immediate dopamine signals were sometimes seen after ejection of L-DOPA. This suggests an additional form of conversion of L-DOPA to dopamine.

Taken together, L-DOPA can be converted to dopamine in dopamine-depleted striatum and be releases as dopamine upon potassium-stimulation. The conversion is possible to occur in nerve fibers or tissues other than dopaminergic. These findings elucidate the conversion of L-DOPA to dopamine and are of importance for better understanding of L-DOPA-induced dyskinesias.

ACKNOWLEDGEMENTS

Firstly, I would like to thank Ingrid Strömberg for being a great mentor and always believing in me. You are a true source of inspiration! I further would like to thank our collaborators in USA and Sweden for help and nice work.

I also thank:
Elisabet Berglöf for being helpful and a great co-worker, and for your deep thoughts about feet. Franziska Marschinke for collaboration, sense of humor and for enduring my baby german. Martin Lundblad, for your patience with me and the e-chem and for being a great prank monkey. Anna Rehnmark for fun times and for being the master of A-solutions. Nina Nevalainen, for bringing new spirit and long nails into the lab. Mikael Andersson, for teaching me everything about the basal ganglia, or at least trying. Heather Boger for collaboration and for introducing me to the fun world of American semi-manufactured food.

Anna Nilsson, the lab-love of my life, I could not have done this without you! Or…I could, but it wouldn't have been the same. Mattias Olsson, a.k.a. Bo, for drilling me with "högskoleprovsord" and withstanding my harassments. Åsa Stenberg, Ing-Marie Sundqvist, and Natalia Gustavsson for nice atmosphere and conversations. Sven Hagnerud for fun and often interesting times during my first years at IMB. Liselotte Vesterlund for information about the life as a graduate student.

Janove Sehlin, Per Lindström, Solveig Persson-Sjögren, and Gerd Larsson-Nyrén for teaching me the basics of histology. Per-Arne Oldenborg, for being joyful and for telling Galenskaparna-jokes. Also thanks to all other staff at IMB for assistance and making IMB a nice working environment.

Old and new friends, for helping me endure the time outside the lab… I need you all. My darling Patrik, for help and encouragement, love you! Finally, I wish to thank my wonderful family for supporting me over the years. Ni är bäst!

REFERENCES

Ahn, Y.H., Bensadoun, J.C., Aebischer, P., Zurn, A.D., Seiger, A., Bjorklund, A., Lindvall, O., Wahlberg, L., Brundin, P., Kaminski Schierle, G.S., 2005. Increased fiber outgrowth from xeno-transplanted human embryonic dopaminergic neurons with co-implants of polymer-encapsulated genetically modified cells releasing glial cell line-derived neurotrophic factor. Brain Res Bull. 66**,** 135-42.

Albin, R.L., Young, A.B., Penney, J.B., 1989. The functional anatomy of basal ganglia disorders. Trends Neurosci. 12**,** 366-375.

Alexander, G.E., DeLong, M.R., Strick, P.L., 1986. Parallel organization of functionally segregated circuits linking basal ganglia and cortex. Ann. Rev. Neurosci. 9**,** 357-381.

Altman, J., Bayer, S.A., 1981. Development of the brain stem in the rat. V. Thymidine-radiographic study of the time of origin of neurons in the midbrain tegmentum. J. Comp. Neurol. 198**,** 677-716.

Arai, R., Karasawa, N., Geffard, M., Nagatsu, I., 1995. L-DOPA is converted to dopamine in serotonergic fibers of the striatum of the rat: a double-labeling immunofluorescence study. Neurosci Lett. 195**,** 195-8.

Backlund, E.-O., Granberg, P.O., Hamberger, B., Knutsson, E., Mårtensson, A., Sedvall, G., Seiger, Å., Olson, L., 1985. Transplantation of adrenal medullary tissue to striatum in parkinsonism. First clinical trials. J. Neurosurg. 62**,** 169-173.

Barbeau, A., 1961. Biochemistry of Parkinson's disease. Int. Congr. Series. 38**,** 152-153.

Barker, R.A., Dunnett, S.B., Faissner, A., Fawcett, J.W., 1996. The time course of loss of dopaminergic neurons and the gliotic reaction surrounding grafts of embryonic mesencephalon to the striatum. Exp. Neurol. 141**,** 79-93.

Bartheld, C.S., 2004. Axonal transport and neuronal transcytosis of trophic factors, tracers, and pathogens. J. Neurobiol. 58**,** 295-314.

Bartholini, G., Pletscher, A., 1968. Cerebral accumulation and metabolism of C 14-DOPA after selective inhibition of pheripheral decarboxylase. J. Pharmacol. Exp. Ther. 161**,** 14-20.

Bendick, J., 2002. Galen and the gateway to medicine, Vol.

Berger, K., Przedborski, S., Cadet, J.L., 1991. Retrograde degeneration of nigrostriatal neurons induced by intrastriatal 6-hydroxydopamine injection in rats. Brain Res. Bull. 26**,** 301-307.

Birkmayer, W., Hornykiewicz, O., 1961. Der 1, 3, 4-dioxyphenylalanin (L-DOPA) -effekt bei der parkinson-akinesia. Klin. Wochenschr. 73**,** 787-788.

Björklund, A., Stenevi, U., 1979. Reconstruction of the nigrostriatal dopamine pathway by intracerebral nigral transplants. Brain Res. 177**,** 555-560.

Björklund, A., Stenevi, U., Dunnett, S.B., Iversen, S.D., 1981. Functional reactivation of the deafferented neostriatum by nigral transplants. Nature. 289**,** 497-499.

Blum, D., Torch, S., Lambeng, N., Nissou, M., Benabid, A.L., Sadoul, R., Verna, J.M., 2001. Molecular pathways involved in the neurotoxicity of 6-OHDA, dopamine and MPTP; contribution to the apoptotic theory in Parkinson's disease. Prog. Neurobiol. 65**,** 135-172.

Boger, H.A., Middaugh, L.D., Huang, P., Zaman, V., Smith, A.C., Hoffer, B.J., Tomac, A.C., Granholm, A.C., 2006. A partial GDNF depletion leads to earlier age-related deterioration of motor function and tyrosine hydroxylase expression in the substantia nigra. Exp Neurol. 202**,** 336-47.

Bolam, J.P., Freund, T.F., Björklund, A., Dunnett, S.B., Smith, A.D., 1987. Synaptic input and local output of dopaminergic neurons in grafts that functionally reinnervate the host striatum. Exp. Brain Res. 68**,** 131-146.

Braak, H., Del Tredici, K., Rüb, U., de Vos, R.A., Jansen Steur, N.E., Braak, E., 2003. Staging of brain pathology related to sporadic Parkinson's disease. Neurobiol. Aging. 24**,** 197-211.

Bresjanac, M., Antaur, G., 2000. Reactive astrocytes of the quinolinic acid-lesioned rat striatum express GFRα1 as well as GDNF *in vivo*. Exp. Neurol. 164**,** 53-59.

Buj-Bello, A., Adu, J., Pinon, L., Horton, A., Thompson, J., Rosenthal, A., Chinchetru, M., Buchman, V., Davies, A., 1997. Neurturin responsiveness requires a GPI-linked receptor and the Ret receptor tyrosine kinase. Nature. 387**,** 721-724.

Cadelli, D.S., Bandtlow, C.E., Schwab, M.E., 1992. Oligodendrocyte- and myelin-associated inhibitors of neurite outgrowth: their involvement in the lack of CNS regeneration. Exp. Neurol. 1992**,** 189-192.

Carlsson, A., Lindqvist, M., Magnusson, T., 1957. 3, 4-dihydroxyphenylalanine and 5-hydroxytryptophan as reserpine antagonists. Nature. 180.

Carlsson, A., Lindqvist, M., Magnusson, T., Waldeck, B., 1958. On the presence of 3-hydroxytyramine in brain. Science. 127.

Carlsson, T., Carta, M., Winkler, C., Bjorklund, A., Kirik, D., 2007. Serotonin neuron transplants exacerbate L-DOPA-induced dyskinesias in a rat model of Parkinson's disease. J Neurosci. 27**,** 8011-22.

Carta, M., Lindgren, H.S., Lundblad, M., Stancampiano, R., Fadda, F., Cenci, M.A., 2006. Role of striatal L-dopa in the production of dyskinesia in 6-hydroxydopamine lesioned rats. J. Neurochem. 96**,** 1718-1727.

Cenci, M.A., Lee, C.S., Björklund, A., 1998. L-dopa-induced dyskinesia in the rat is associated with striatal overexpression of prodynorphin- and glutamatic acid decarboxylase mRNA. Eur. j. Neurosci. 10**,** 2694-2706.

Chronister, R.B., Sikes, R.W., Wood, J., DeFrance, J.F., 1980. The pattern of termination of ventral tegmental afferents into nucleus accumbens: an anterograde HRP analysis. Neurosci Lett. 17**,** 231-5.

Chung, S., Hedlund, E., Hwang, M., Kim, D.W., Shin, B.-S., Hwang, D.-Y., Kang, U.J., Isacson, O., Kim, K.-S., 2005. The homeodomain transcription factor Pitx3 facilitates differentiation of mouse embryonic stem cells into AHD2-expressing dopaminergic neurons. Mol. Cell Neurosci. 28**,** 241-252.

Clarke, D., Brundin, P., Strecker, R., Nilsson, O., Björklund, A., Lindvall, O., 1988. Human fetal dopamine neurons grafted in a rat model of Parkinson’s

disease: Ultratructural evidence for synapse formation using tyrosine hydroxylase immunoctyochemistry. Exp Brain Res. 73**,** 115-126.
Cochen, V., Ribeiro, M.J., Nguyen, J.P., Gurruchaga, J.M., Villafane, G., Loc'h, C., 2003. Transplantation in Parkinson's disease: PET changes correlate with the amount of grafted tissue. Mov. Disord. 18**,** 928-932.
Cohen, S., 1959. Purification of nerve growth factor from snake venom. J. Biol. Chem. 234**,** 1129-1137.
Cohen, S., 1960. Purification of nerve growth promoting protein from mouse salivary gland and its neurocytotoxic antiserum. Proc. Natl. Acad. Sci. 46**,** 302-311.
Conner, J.M., Lauterborn, J.C., Gall, C.M., 1998. Anterograde transport of neurotrophin proteins in the CNS-reassessment of the neurotrophic hypothesis. Rev. Neurosci. 9**,** 91-103.
Correia, A.S., Anisimov, S.V., Li, J.Y., Brundin, P., 2005. Stem cell-based therapy for Parkinson's disease. Ann. Med. 37**,** 487-498.
Cotzias, G.C., van Woert, M.H., Schiffer, L.M., 1967. Aromatic amino acids and modification of parkinsonism. New Engl. J. Med. 276**,** 374-379.
Creange, A., Barlovatz-Meimon, G., Gherardi, R.K., 1997. Cytokines and peripheral nerve disorders. Eur. Cytokine Netw. 8**,** 145-151.
Crossman, A.R., 1989. Neural mechanisms in disorders of movement. Comp. Biochem. Physiol. A. 93**,** 141-149.
Dahlström, A., Fuxe, K., 1964. Evidence for the existence of monoamine-containing neurons in the central nervous system. I. Demonstration of monoamines in the cell bodies of the brain stem neurons. Acta Physiol Scand. Suppl. 232. 62**,** 1-55.
Date, I., Yoshimoto, Y., Imaoka, T., Miyoshi, Y., Gohda, Y., Furuta, T., Asari, S., Ohmoto, T., 1993. Enhanced recovery of the nigrostriatal dopaminergic system in MPTP-treated mice following intrastriatal injection of basic fibroblast growth factor in relation to aging. Brain Research. 621**,** 150-154.
DeLong, M.R., 1990. Primate models of movement disorders of basal ganglia origin. Trends Neurosci. 13**,** 281-285.
DiStefano, P.S., Friedman, B., Radziejewski, C., Alexander, C., Boland, P., Schick, C.M., Lindsay, R.M., Wiegand, S.J., 1992. The neurotrophins BDNF, NT-3, and NGF display distinct patterns of retrograde axonal transport in peripheral and central neurons. Neuron. 8**,** 983-993.
Dunner, D.L., Brodie, K.H., Goodwin, F.K., 1971. Plasma DOPA response to levodopa administration in man: effects of a peripheral decarboxylase inhibitor. Clin. Pharmacol. Exp. Ther. 12**,** 212-217.
Dunnett, S.B., Björklund, A., 1992. Staging and dissection of rat embryos. In: Neural transplantation, a practical approach. Vol., ed.^eds. Oxford Univ. Press, New York, pp. 1-19.
Durbec, P., Marcos-Gutierrez, C.V., Kilkenny, C., Grigoriou, M., Wartiowaara, K., Suvanto, P., Smith, D., Ponder, B., Costantini, F., Saarma, M., Sariola, H., Pachnis, V., 1996. GDNF signaling through the Ret receptor tyrosine kinase. Nature. 381**,** 789-793.
Ehringer, H., Hornykiewicz, O., 1960. Verteilung von noradrenalin und dopamin (3-hydroxytyramin) im gehirn des menschen und ihr verhalten bei erkrankungen des extrapyramidalen systems. Klin. Wschr. 38**,** 1236-1239.

Eriksen, J.L., Dawson, T.M., Dickson, D.W., Petrucelli, L., 2003. Caught in the act: alpha-synuclein is the culprit in Parkinson's disease. Neuron. 40**,** 453-456.

Fahn, S., 2003. Description of Parkinson's disease as a clinical syndrome. Ann. N.Y. Acad. Sci. . 991**,** 1-14.

Falck, B., Hillarp, N.-Å., Thieme, G., Torp, A., 1962. Fluorescence of catecholamines and related compounds condenced with formaldehyde. J. Histochem. Cytochem. 10**,** 348-354.

Farrer, M.J., 2006. Genetics of Parkinson's disease: paradigm shifts and future prospects. Nat. Rev. Genet. 7**,** 306-318.

Faull, R.L., Laverty, R., 1969. Changes in dopamine levels in the corpus striatum following lesions in the substantia nigra. Exp. Neurol. 23**,** 332-340.

Fearnley, J.M., Lees, A.J., 1991. Ageing and Parkinson's disease: substantia nigra regional selectivity. Brain. 114**,** 2283-2301.

Fisher, L.J., Young, S.J., Tepper, J.M., Groves, P.M., Gage, F.H., 1991. Electrophysiological characteristics of cells within mesencephalon suspension grafts. Neurosci. 40**,** 109-122.

Förander, P., Broberger, I., Strömberg, I., 2001. Glial cell line-derived neurotrophic factor induces nerve fibre formation in primary cultures of adrenal chromaffin cells. Cell Tissue Res. 305**,** 43-51.

Foster, G., Schultzberg, M., Hökfelt, T., Goldstein, M., Hemmings, H.C., Ouimet, C.C., Walaas, S.I., Greengard, P., 1988. Ontogeny of the dopamine and cyclic adenosine-3´:5´-monophosphate-regulated phosphoprotein (DARPP-32) in the pre- and postnatal mouse central nervous system. Int. J. Dev. Neurosci. 6**,** 367-386.

Freed, C., Greene, P., Breeze, R., Tsai, W., DuMouchel, W., Kao, R., Dillon, S., Winfield, H., Culver, S., Trojansowski, J., Eidelberg, D., Fahn, S., 2001. Transplantation of embryonic dopamine neurons for severe Parkinson's disease. N Engl. J. Med. 344**,** 710-719.

Freed, W.J., Perlow, M.J., Karoum, F., Seiger, Å., Olson, L., Hoffer, B.J., Wyatt, R.J., 1980. Restoration of dopaminergic function by grafting fetal rat substantia nigra to the caudate nucleus: long-term behavioral, biochemical, and histochemical studies. Ann. Neurol. 8**,** 510-519.

Friedemann, M., Gerhardt, G.A., 1992. Regional effects of aging on dopaminergic function in the Fischer-344 rat. Neurobiol. Aging. 13**,** 325-332.

Gähwiler, B.H., Capogna, M., Debanne, D., McKinney, R.A., Thompson, S.M., 1997. Organotypic slice cultures: A technique has come of age. Trends in Neurosci. 20**,** 471-477.

Gates, M.A., Torres, E.M., White, A., Fricker-Gates, R.A., Dunnett, S.B., 2006. Re-examining the ontogeny of substantia nigra dopamine neurons. Eur. J. Neurosci. 23**,** 1384-1390.

Georgievska, B., Kirik, D., Rosenblad, C., Lundberg, C., Bjorklund, A., 2002. Neuroprotection in the rat Parkinson model by intrastriatal GDNF gene transfer using a lentiviral vector. Neuroreport. 13**,** 75-82.

Gerfen, C.R., Baimbridge, K.G., Miller, J.J., 1985. The neostriatal mosaic: compartmental distribution of calcium-binding protein and parvalbumin in

the basal ganglia of the rat and monkey. Proc Natl Acad Sci U S A. 82**,** 8780-4.
Gerfen, C.R., Baimbridge, K.G., Thibault, J., 1987. The neostriatal mosaic: III. Biochemical and developmental dissociation of patch-matrix mesostriatal systems. J Neurosci. 7**,** 3935-44.
Gerfen, C.R., Wilson, C.J., 1996. The Basal Ganglia. In: Handbook of chemical neuroanatomy: Integrated systems of the CNS, part III. Vol. 12, L.W. Swanson, A. Björklund, T. Hökfelt, ed.^eds. Elsevier Science B.V, Amsterdam, pp. 371-468.
Gerhardt, G.A., Oke, A.F., Nagy, G., Moghaddam, B., Adams, R.N., 1984. Nafion-coated electrodes with high selectivity for CNS electrochemistry. Brain Res. 190**,** 390-395.
German, D.C., Liang, C.L., 1993. Neuroactive peptides exist in the midbrain dopaminergic neurons that contain calbindin-D28k. Neuroreport. 4**,** 491-4.
Giacobini, M.M.J., Strömberg, I., Almström, S., Cao, Y., Olson, L., 1993. Fibroblast growth factors enhance dopamine fiber formation from nigral grafts. Dev. Brain Res. 75**,** 65-73.
Gibb, W., Lees, A.J., 1991. Anatomy, pigmentation, ventral and dorsal subpopulations of the substantia nigra, and differential cell death in Parkinson's disease. J. Neurol. Neurosurg. Psychiatry. 54**,** 388-396.
Gill, S.S., Patel, N.K., Hotton, G.R., O'Sullivan, K., McCarter, R., Bunnage, M., Brooks, D.J., Svendsen, C.N., Heywood, P., 2003. Direct brain infusion of glial cell line-derived neurotrophic factor in Parkinson disease. Nat. Med. 9**,** 589-598.
Granérus, A.-K., 1978. Factors influencing the occurence of "on-off" symptoms during long-term treatment with l-dopa. Acta Med. Scand. 203**,** 75-85.
Granholm, A.-C., Mott, J.L., Bowenkamp, K., Eken, S., Henry, S., Hoffer, B.J., Lapchak, P.A., Palmer, M.R., van Horne, C., Gerhardt, G.A., 1997. Glial cell line-derived neurotrophic factor improves survival of ventral mesencephalic grafts to the 6-hydroxydopamine lesioned striatum. Exp. Brain Res. 116**,** 29-38.
Granholm, A.-C., Reyland, M., Albeck, D., Sanders, L., Gerhardt, g., Hoerning, G., Shen, L., Westphal, H., Hoffer, B., 2000. Glial cell line-derived neurotrophic factor is essential for postnatal survival of midbrain dopamine neurons. J. Neurosci. 20**,** 3182-3190.
Granholm, A.-C.E., Curtis, M., Diamond, D.M., Branch, B.J., Heman, K.L., Rose, G.M., 1996. Development of an intact blood-brain barrier in brain tissue transplants is dependent on the site of transplantation. Cell Transplant. 5**,** 305-314.
Graybiel, A.M., Ragsdale Jr, C.W., 1978. Histochemically distinct compartments in the striatum of human, monkey, and cat demonstrated by acetylcholinesterase staining. Proc. Natl. Acad. Sci. USA. 75**,** 5723-5726.
Hagell, P., Schrag, A., Piccini, P., Jahanshahi, M., Brown, R., Rehncrona, S., 1999. Sequential bilateral transplantation in Parkinson's disease: effects of the second graft. Brain. 122**,** 1121-1132.
Hagell, P., Piccini, P., Björklund, A., Brundin, P., Rehncrona, S., Widner, H., Crabb, L., Pavese, N., Oertel, W., Quinn, N., Brooks, D., Lindvall, O.,

2002. Dyskinesias following neural transplantation in Parkinson's disease. Nat. Neurosci. 5**,** 627-628.
Hanaway, J., McConnell, J.A., Netsky, M.G., 1971. Histogenesis of the substantia nigra, ventral tegmental area of Tsai and interpeduncular nucleus: an autoradiographic study of the mesencephalon in the rat. J. Comp. Neurol. 142**,** 59-74.
Heikkila, R.D., Shapiro, B.S., Duvoisin, R.C., 1981. The relationship between loss of dopamine nerve terminals, striatal ^{3}H-spiroperidol binding and rotational behavior in unilaterally 6-OHDA lesioned rats. Brain Res. 211**,** 285-292.
Heins, N., Malatesta, P., Cecconi, F., Nakafuku, M., Tucker, K., Hack, M., P, C., Barde, Y.-A., Götz, M., 2002. Glial cells generate neurons: the role of the transcription factor PAx6. Nature Neurosci. 5**,** 308-315.
Hernández-Montiel, H., Tamariz, E., Sandoval-Minero, M., Varela-Echavirría, A., 2008. Semaphorins 3A, 3C, and 3F in mesencephalic dopaminergic axon pathfinding. J. Comp. Neurol. 506**,** 387-397.
Herrera-Marschitz, M., Ungerstedt, U., 1984. Evidence that apomorphine and pergolide induce rotations in rats by different actions on D1 and D2 receptor sites. Eur. J. Pharmacol. 6**,** 165-176.
Hidalgo, A., Urban, J., Brand, A.H., 1995. Target ablation of glia disrupts axon tract formation in the Drosophila CNS. Development. 121**,** 3703-3712.
Hidalgo, A., Booth, G.E., 2000. Glia dictate pioneer axon trajectories in the *Drosophila* embryonic CNS. Development. 127**,** 393-402.
Hoffman, A.F., Lupica, C.R., Gerhardt, G.A., 1998. Dopamine transporter activity in the substantia nigra and striatum assessed by high-speed chronoamperometric recordings in brain slices. J. Pharmacol. 287**,** 487-496.
Hökfelt, T., Ungerstedt, U., 1969. Electron and fluorescence microscopical studies on the nucleus caudatus putamen of the rat after unilateral lesions of ascending nigro-neostriatal dopamine neurons. Acta Physiol Scand. 76**,** 415-26.
Hökfelt, T., Fuxe, K., Goldstein, M., 1973. Immunohistochemical localization of aromatic L-amino acid decarboxylase (DOPA decarboxylase) in central dopamine and 5-hydroxytryptamine nerve cell bodies of the rat. Brain Res. 53**,** 175-180.
Horger, B.A., Nishimura, M.C., Armanini, M.P., Wang, L.C., Poulsen, K.T., Rosenblad, C., Kirik, D., Moffat, B., Simmons, L., Johnson, E.J., Milbrandt, J., Rosenthal, A., Björklund, A., Vandlen, R., Hynes, M.A., Phillips, H.S., 1998. Neurturin exerts potent actions on survival and function of midbrain dopaminergic neurons. J. Neurosci. 18**,** 4929-4937.
Huang, S., 1990. Some characteristics of rat nigrostriatal dopaminergic neuroconnection during development - a combined immunocytochemical and electron-microscopic study. Sci China, Ser B Chem Life Sci Earth Sci. 33**,** 1326-1333.
Hudson, J., Granholm, A.-C., Gerhardt, G.A., Henry, M.A., Hoffman, A., Biddle, P., Leela, N.S., Mackerlova, L., Lile, J.D., Collins, F., Hoffer, B.J., 1995. Glial cell line-derived neurotrophic factor augments midbrain dopaminergic circuits *in vivo*. Brain Res. Bull. 36**,** 425-432.

Hudson, J.L., van Horne, C.G., Strömberg, I., Brock, S., Clayton, J., Masserano, J., Hoffer, B.J., Gerhardt, G.A., 1993. Correlation of apomorphine- and amphetamine-induced turning with nigrostriatal dopamine content in unilateral 6-hydroxydopamine lesioned rats. Brain Res. 626**,** 167-174.

Hussain, G., Manyam, B.V., 1997. Mucuna Pruriens proves more effective than L-DOPA in Parkinson's disease animal model. Phytotherapy Res. 11**,** 419-423.

Hyman, C., Hofer, M., Barde, Y.-A., Juhasz, M., Jancopoulos, G., Squinto, S., Lindsay, R., 1991. BNDF is a neurotrophic factor for dopaminergic neurons of the substantia nigra. Nature. 350**,** 230-232.

Hynes, M.A., Poulsen, K., Armanini, M., Berkemeier, L., Phillips, H., Rosenthal, A., 1994. Neurotrophin-4/5 is a survival factor for embryonic midbrain dopaminergic neurons in enriched cultures. J. Neurosci. Res. 37**,** 144-154.

Jacobsen, B., Gramsbergen, J.B., Møller Dall, A., Rosenblad, C., Zimmer, J., 2005. Characterization of organotypic ventral mesencephalic cultures from embryonic mice and protection against MPP^+ toxicity by GDNF. Eur. J. Neurosci. 21**,** 2939-2948.

Jaumotte, J.D., Zigmond, M.J., 2005. Dopaminergic innervation of forebrain by ventral mesencephalon in organotypic slice co-cultures: Effects of GDNF. Mol. Brain Res. 134**,** 139-146.

Jellinger, K.A., Paulus, W., 1992. Clinico-pathological correlations in Parkinson's disease. Clin. Neurol. Neurosurg. 94**,** 86-88.

Johansson, S., Strömberg, I., 2002. Guidance of dopaminergic neuritic growth by immature astrocytes in organotypic cultures of rat fetal ventral mesencephalon. J. Comp. Neurol. 443**,** 237-249.

Johansson, S., Strömberg, I., 2003. Fetal lateral ganglionic eminence attracts one of two morphologically different types of tyrosine hydroxylase-positive nerve fibers formed by cultured ventral mesencephalon. Cell Transplant. 12**,** 243-255.

Kalsbeek, A., Voorn, P., Buijs, R.M., Pool, C.W., Uylings, H.B., 1988. Development of the dopaminergic innervation in the prefrontal cortex of the rat. J Comp Neurol. 269**,** 58-72.

Kalsbeek, A., Voorn, P., Buijs, R.M., 1992. Development of dopamine-containing systems in the CNS. In: Ontogeny of transmitters and peptides in the CNS. Vol. 10, A. Björklund, T. Hökfeldt, M. Tohyama, ed.^eds. Elsevier Science Publishers B.V.

Kapfhammer, J.P., Schwab, M.E., Schneider, G.E., 1992. Antibody neutralization of neurite growth inhibitors from oligodendrocytes results in expanded pattern of postnatally sprouting retinocollicular axons. J Neurosci. 12**,** 2112-2119.

Kinameri, E., Matsuoka, I., 2003. Autocrine action of BPM2 regulates expression of GDNF-mRNA in sciatic Schwann cells. Mol. Brain Res. 117**,** 221-227.

Kirik, D., Rosenblad, C., Bjorklund, A., Mandel, R.J., 2000. Long-term rAAV-mediated gene transfer of GDNF in the rat Parkinson's model: intrastriatal

but not intranigral transduction promotes functional regeneration in the lesioned nigrostriatal system. J Neurosci. 20**,** 4686-700.
Kish, S.J., Shannak, K., Hornykiewicz, O., 1988. Uneven pattern of dopamine loss in the striatum of patients with idiopathic Parkinson's disease. Pathophysiologic and clinical implications. New Engl. J. Med. 318**,** 876-880.
Kissinger, P.T., Hart, J.B., Adams, R.N., 1973. Voltammetry in brain tissue - a new neurophysiological measurement. Brain Res. 55**,** 209-213.
Kordower, J.H., Freeman, T.B., Snow, B.J., Vingerhoets, F.J.G., Mufson , E.J., Sandberg, P.R., Hauser, R.A., Smith, D.A., Nauert, G.M., Perl, D.P., Olanow, C.W., 1995. Neuropathological evidence of graft survival and striatal reinnervation after transplantation of fetal mesencephalic tissue in a patient with Parkinson's disease. N. Engl. J. Med. 332**,** 1118-1124.
Kordower, J.H., Freeman, T.B., Chen, E.Y., Mufson, E.J., Sandberg, P.R., Hauser, R.A., Snow, B., Olanow, C.W., 1998. Fetal nigral grafts survive and mediate clinical benfit in a patient with Parkinson's disease. Mov. Disord. 13**,** 383-93.
Kordower, J.H., Palfi, S., Chen, E.Y., Ma, S.Y., Sendera, T., Cochran, E.J., Mufson, E.J., Penn, R., Goetz, C.G., Comella, C.D., 1999. Clinicopathological findings following intraventricular glial-derived neurotrophic factor treatment in a patient with Parkinson's disease. Ann. Neurol. 46**,** 419-424.
Lang, A.E., Gill, S.S., Patel, N.K., Lozano, A.M., Nutt, J.G., Penn, R., Brooks, D.J., Hotton, G.R., Moro, E., Heywood, P., Brodsky, M.A., Burchiel, K.J., Kelly, P., Dalvi, A., Scott, B., Stacy, M., Turner, D., Wooten, G.F., Elias, W.J., Laws, E.R.J., Dhawan, V., Stoessl, A.J., Matcham, J., Coffrey, R.J., Traub, M., 2006. Randomized controlled trial of intraputamenal glial cell line-derived neurotrophic factor infusion in Parkinson's disease. Ann. Neurol. 58**,** 459-466.
Lauder, J., Bloom, F., 1974. Ontogeny of monoamine neurons in the locus coeruleus, raphe nuclei and substantia nigra of the rat. J. Comp. Neurol. 155**,** 469-482.
Lee, C.S., Cenci, M.A., Schulzer, M., Björklund, A., 2000. Embryonic ventral mesencephalic grafts improve levodopa-induced dyskinesia in a rat model of Parkinson's disease. Brain. 123**,** 1365-1379.
Lester, J., Fink, S., Aronin, N., DiFiglia, M., 1993. Colocalization of D1 and D2 dopamine receptor mRNAs in striatal neurons. Brain Res. 621**,** 106-110.
Levi-Montalcini, R., Hamburger, V., 1953. A diffusible agent of mouse sarcoma producing hyperplasia of sympathetic ganglia and hyperneurotization of viscera in the chick embryo. J. Exp. Chem. 123**,** 233-287.
Lewy, F., 1912. Paralysis agitans. I. Pathologische anatomie. In: Handbuch der neurologie. Vol., M. Lewandowsky, ed.^eds. Springer, Berlin, pp. 920-933.
Lin, L.-F.H., Doherty, D.H., Lile, J.D., Bektesh, S., Collins, F., 1993. GDNF: A glial cell line-derived neurotrophic factor for midbrain dopaminergic neurons. Science. 260**,** 1130-1132.

Lindvall, O., Backlund, E.-O., Farde, L., Sedvall, G., Freedman, R., Hoffer, B., Nobin, A., Seiger, Å., Olson, L., 1987. Transplantation in Parkinson's disease: Two cases of adrenal medullary grafts to the putamen. Ann. Neurol. 22**,** 457-468.

Lindvall, O., Rehncrona, S., Gustaavii, B., Brundin, P., Åstedt, B., Widner, H., Lindholm, T., Björklund, A., Leenders, K., Rothwell, J., Frackowiak, R., Marsden, C.D., Johnels, B., Steg, G., Freedman, R., Hoffer, B.J., Seiger, Å., Strömberg, I., Bygdeman, M., Olson, L., 1988. Fetal dopamine-rich mesencephalic grafts in Parkinson's disease. Lancet. 8626-8627**,** 1483-1484.

Love, S., Plaha, P., Patel, N.K., Hotton, G.R., Brooks, D.J., Gill, S.S., 2005. Glial cell line-derived neurotrophic factor induces neuronal sprouting in human brain. Nat. Med. 11**,** 703-704.

Lovenberg, W., Weissbach, H., Udenfriend, S., 1962. Aromatic L-amino acid decarboxylase. J. Biol. Chem. 237**,** 89-93.

Lundblad, M., Andersson, M., Winkler, C., Kirik, D., Wierup, N., Cenci, M.A., 2002. Pharmacological validation of behvioural measures of akinesia and dyskinesia in a rat model of Parkinson's disease. Eur. J. Neurosci. 15**,** 120-132.

Luthman, J., Bolioli, B., Tsutsumi, T., Verhofstad, A., Jonsson, G., 1987. Sprouting of striatal serotonin nerve terminals following selective lesions of nigro-striatal dopamine neurons in neonatal rat. Brain Res Bull. 19**,** 269-74.

Madrazo, I., Leon, V., Torres, C., 1988. Transplantation of fetal substantia nigra and adrenal medulla to the nucleus caudatus in two patients with Parkinson's disease. New Engl. J. Med. 318.

Mahalik, T.J., Finger, T.E., Strömberg, I., Olson, L., 1985. Substantia nigra transplants into denervated striatum of the rat: ultrastructure of graft and host interconnections. J. Comp. Neurol. 260**,** 60-70.

Malatesta, P., Hack, M., Hartfuss, E., Kettenmann, H., Klinkert, W., Kirchhoff, F., Gotz, M., 2003. Neuronal or glial progeny: regional differences in radial glia fate. Neuron. 37**,** 751-764.

Mann, D.M., Yates, P.O., 1983a. Pathological basis for neurotransmitter changes in Parkinson's disease. Neuropathol. Appl. Neurobiol. 9**,** 3-19.

Mann, D.M.A., Yates, P.O., 1983b. Possible role of neuromelanin in the patogenesis of Parkinson's disease. Mech. Ageing Dev. 20**,** 193-203.

Marchand, R., Poirer, L.J., 1983. Isthmic origin of neurons of the rat substantia nigra. Neurosci. 9**,** 373-381.

Maries, E., Kordower, J.H., Chu, Y., Collier, T.J., Sortwell, C.E., Olaru, E., Shannon, K., Steece-Collier, K., 2006. Focal not widespread grafts induce novel dyskinetic behavior in parkinsonian rats. Neurobiol Dis. 21**,** 165-80.

Marsden, C.D., 1990. Parkinson's disease. Lancet. 335**,** 948-952.

Mayer, E., Fawcett, J., Dunnett, S., 1993. Basic fibroblast growth factor promotes the survival of embryonic ventral mesencephalic dopaminergic neurons. Effects on nigral transplants in vivo. Neurosci. 56**,** 389-98.

McCaffery, P., Drager, U.C., 1994. High levels of a retinoic acid-generating dehydrogenase in the meso-telencephalic dopamine system. Proc. Natl. Acad. Sci. USA. 91**,** 7772-7776.

Melamed, E., Hefti, F., Wurtman, R.J., 1980. Decarboxylation of exogenous L-DOPA in rat striatum after lesions of the dopaminergic nigrostriatal neurons: the role of striatal capillaries. Brain Res. 198**,** 244-8.
Merkle, F., Tramontin, A., Garcia-Verdugo, J., Alvarez-Buylla, A., 2004. Radial glia give rise to adult neural stem cells in the subventricular zone. Proc. Natl. Acad. Sci. 101**,** 17528-17532.
Meyer, M., Zimmer, J., Seiler, R.W., Widmer, H.R., 1999. GDNF increases the density of cells containing calbindin but not of cells containing calretinin in cultured rat and human fetal nigral tissue. Cell Transplant. 8**,** 25-36.
Miller, D.W., Abercrombie, E.D., 1999. Role of high-affinity dopamine uptake and impulse activity in the appearance of extracellular dopamine in striatum after administration of exogenous L-DOPA: studies in intact and 6-hydroxydopamine-treated rats. J Neurochem. 72**,** 1516-22.
Moore, M.W., Klein, R.D., Fariñas, I., Sauer, H., Armanini, M., Phillips, H., Reichert, L.F., Ryan, A.M., Carever-Moore, K., Rosenthal, A., 1996. Renal and neuronal abnormalities in mice lacking GDNF. Nature. 382**,** 76-79.
Mufson, E.J., Kroin, J.S., Sendera, T.J., Sobreviela, T., 1999. Distribution and retrograde transport of trophic factors in the central nervoussystem: functional implications for the treatment of neurodegenerative diseases. Prog. Neurobiol. 57**,** 451-484.
Nagy, G., Gerhardt, G.A., Oke, A.F., Rice, M.E., Adams, R.N., 1985. Ion exchange and transport of neurotransmitters in nafion films on conventional and microelectrode surface. J. Electroanal. Chem. 188**,** 85-94.
Nakajima, K., Hida, H., Shimano, Y., Fujimoto, I., Hashitani, T., Kumazaki, M., Sakurai, T., Nishino, H., 2001. GDNF is a major component of trophic activity in DA-depleted striatum for survival and neurite extension of DAergic neurons. Brain Res. 916**,** 76-84.
Nakano, I., Hirano, A., 1984. Parkinson's disease: neuron loss in the nucleus basalis without concomitant Alzheimer's disease. Ann. Neurol. 15**,** 415-418.
Narabayashi, H., 1990. Surgical treatment in the levodopa era. In: Parkinson's disease. Vol., GS, ed.^eds. Chapman and Hall medical, London, pp. 597-646.
Nirenberg, M.J., Liu, Y., Peter, D., Edwards, R.H., Pickel, V.M., 1995. The vesicular monoamine transporter 2 is present in small synaptic vesicles and preferentially localizes to large dense core vesicles in rat solitary tract nuclei. Proc Natl Acad Sci U S A. 92**,** 8773-7.
Nutt, J.G., Burchiel, K.J., Comella, C.L., Jankovic, J., Lang, A.E., Laws, E.R.J., Lozano, A.M., Penn, R.D., Simpson, R.K.J., Stacy, M., Wooten, G.F., 2003. Randomized, double-blind trial of glial cell line-derived neurotrophic factor (GDNF) in PD. Neurology. 60**,** 69-73.
Nyberg, P., Nordberg, A., Wester, P., Winblad, B., 1983. Dopaminergic deficiency is more pronounced in putamen than in nucleus caudatus in Parkinson’s disease. Neurochem. Pathol. 1**,** 193-202.
Olanow, C., Goetz, C., Kordower, J., Stoessl, A., Sossi, V., Brinn, M., Shannon, K., Nauert, G., Perl, D., Godbold, J., Freeman, T., 2003. A double-blind controlled trial of bilateral fetal nigral transplantation in Parkinson's disease. Ann. Neurol. 54**,** 403-414.

Olanow, C.W., 2007. The pathogenesis of cell death in Parkinson's disease - 2007. Mov. Disord. 22**,** 335-342.
Olson, L., Seiger, Å., 1972. Early prenatal ontogeny of central monoamine neurons in the rat: Fluorescence histochemical observations. Z. Anat. Entwickl.-Gesch. 137**,** 301-316.
Olson, L., Seiger, Å., Fuxe, K., 1972. Heterogeneity of striatal and limbic dopamine innervation: Highly fluorescent islands in developing and adult rats. Brain Res. 44**,** 283-288.
Olson, L., Seiger, Å., Strömberg, I., 1983. Intraocular transplantation in rodents. A detailed account of the procedure and examples of its use in neurobiology with special reference to brain tissue grafting. In: Advances in Cellular Neurobiology. Vol. 4, S. Federoff, L. Hertz, ed.^eds. Academic, New York, pp. 407-442.
Pakzaban, P., Deacon, T.W., Burns, L.H., Isacson, O., 1993. Increased proportion of acetylcholinesterase-rich zones and improve morphological integration in host striatum of fetal grafts derived from the lateral but not the medial ganglionic eminence. Exp. Brain Res. 97**,** 13-22.
Paratcha, G., Ledda, F., Ibanez, C.F., 2003. The neural cell adhesion molecule NCAM is an alternative signaling receptor for GDNF family ligands. Cell. 113**,** 867-879.
Parent, A., Sato, F., Wu, Y., Gauthier, J., Levesque, M., Parent, M., 2000. Organization of the basal ganglia: the importance of axonal collateralization. Trends Neurosci. 23**,** 20-27.
Parish, C.L., Arenas, E., 2007. Stem-cell-based strategies for the treatment of Parkinson's disease. Neurodeg. Dis. 4**,** 339-347.
Parkinson, J., 2002. An essay on the shaking palsy. J. Neuropsychiatry Clin. Neurosci. 14**,** 223-236.
Perese, D.A., Ulman, J., Violoa, J., Ewing, S.E., Bankiewicz, K.S., 1989. A 6-hydroxydopamine-induced selective parkinsonian rat model. Brain Res. 494**,** 285-293.
Perlow, M.J., Freed, W.J., Hoffer, B.J., Seiger, Å., Olson, L., Wyatt, R.J., 1979. Brain grafts reduce motor abnormalities produced by destruction of nigrostriatal dopamine system. Science. 204**,** 643-647.
Peter, D., Liu, Y., Sternini, C., de Giorgio, R., Brecha, N., Edwards, R.H., 1995. Differential expression of two vesicular monoamine transporters. J Neurosci. 15**,** 6179-88.
Piccini, P., Brooks, D.J., Björklund, A., Gunn, R.N., Grasby, P.M., Rimoldi, O., Brundin, P., Hagell, P., Rehncrona, S., Widner, H., Linvall, O., 1999. Dopamine release from nigral transplants visualized in vivo in a Parkinon's patient. Nat. Neurosci. 2**,** 1137-1140.
Piccini, P., Lindvall, O., Björklund, A., Brundin, P., Hagell, P., Ceravolo, R., 2000. Delayed recovery of movement-related cortical function in Parkinson's disease after striatal dopaminergic grafts. Ann. Neurol. 48**,** 689-695.
Pichel, J.G., Shen, L., Sheng, H.Z., Granholm, A.C., Drago, J., Grinberg, A., Lee, E.J., Huang, S.P., Saarma, M., Hoffer, B.J., Sariola, H., Westphal, H., 1996. Defects in enteric innervation and kidney development in mice lacking GDNF. Nature. 382**,** 73-76.

Porter, C.C., Totaro, J.A., Stone, C.A., 1963. Effect of 6-hydroxydopamine and some other compounds on the concentration of norepinephrine in the hearts of mice. J. Pharmacol. Exp. Ther. 140**,** 308-316.

Porter, C.C., Totaro, J.A., Burcin, A., 1965. The relationship between radioactivity and norepinephrine concentrations in the brains and hearts of mice following administration of labeled methyldopa or 6-hydroxydopamine. J. Pharmacol. Exp. Ther. 150**,** 17-22.

Poteryaev, D., Titievsky, A., Sun, Y.F., Thomas-Crusells, J., Lindahl, M., Billaud, M., Arumae, U., Saarma, M., 1999. GDNF triggers a novel Ret-independent Src kinase family-coupled signaling via a GPI-linked GDNF receptor alpha 1. FEBS Lett. 463**,** 63-66.

Przedborski, S., Levivier, M., Jiang, H., Ferreira, M., Jackson-Lewis, V., Donaldson, D., Togasaki, D.M., 1995. Dose-dependent lesions of the dopaminergic nigrostriatal pathway induced by intrastriatal injection of 6-hydroxydopamine. Neurosci. 67**,** 631-647.

Rascol, O., Brooks, D.J., Korczyn, A.D., De Deyn, P.P., Clarke, C.E., Lang, A.E., 2000. A five-year study of the incidence of dyskinesia in patients with early Parkinson's disease who were treated with ropinirole or levodopa. 056 Study Group. N. Engl. J. Med. 342**,** 1484-1491.

Rose, G., Gerhardt, G., Strömberg, I., Olson, L., Hoffer, B., 1985. Monoamine release from dopamine-depleted rat caudate nucleus reinnervated by substantia nigra transplants: An in vivo electrochemical study. Brain Res. 341**,** 92-100.

Sajadi, A., Bensadoun, J.C., Schneider, B.L., Lo Bianco, C., Aebischer, P., 2006. Transient striatal delivery of GDNF via encapsulated cells leads to sustained behavioral improvement in a bilateral model of Parkinson disease. Neurobiol. Dis. 22**,** 119-29.

Sánchez, M.P., Silos-Santiago, I., Frisén, J., He, B., Lira, S.A., Barbacid, M., 1996. Renal agenesis and the absence of enteric neurons in mice lacking GDNF. Nature. 382**,** 70-73.

Sarre, S., De Klippel, N., Herregodts, P., Ebinger, G., Michotte, Y., 1994. Biotransformation of locally applied L-dopa in the corpus striatum of the hemi-parkinsonian rat studied with microdialysis. Naunyn Schmiedebergs Arch Pharmacol. 350**,** 15-21.

Sauer, H., Oertel, W.H., 1994. Progressive degeneration of nigrostriatal dopamine neurons following intrastriatal terminal lesions with 6-hydroxydopamine: a combined retrograde tracing and immunocytochemical study in the rat. Neurosci. 59**,** 401-415.

Sawada, M., Imamura, K., Nagatsu, T., 2006. Role of cytokines in inflammatory process in Parkinson's disease. J. Neural. Transm. Suppl. 70**,** 373-381.

Scatton, B., D'Angio, M., Serrano, A., 1988. An in vivo voltammetric study of the response of mesocortical and mesoaccumbens dopaminergic neurons to environmental stimuli in strains of rats with differing levels of emotionality. Ann N.Y. Acad. Sci. 537**,** 124-137.

Schaar, D.G., Sieber, B.-A., Dreyfus, C.F., Black, I.B., 1993. Regional and cell-specific expression of GDNF in rat brain. Exp. Neurol. 124**,** 368-371.

Schaller, B., Anders, R.H., Huber, A.W., Meyer, M., Pérez-Bouza, A., Ducray, A.D., Seiler, R.W., Widmer, H.R., 2005. Effects of GDNF on differentiation of cultured ventral mesencephalic dopaminergic and non-dopaminergic calretinin-expressing neurons. Brain Res. 1036**,** 163-172.

Schein, J., Hunter, D., Roffler-Tarlov, S., 1998. Girk2 expression in the ventral midbrain, cerebellum, and olfactory bulb and its relationship to the murine mutation weaver. Dev. Biol. 204**,** 432-450.

Schwarting, R.K., Huston, J.P., 1996. The unilateral 6-hydroxydopamine lesion model in behavioral brain research. Prog. Neurobiol. 50**,** 275-331.

Seiger, Å., 1985. Preparation of immature central nervous system regions for transplantation. Vol., ed.^eds. Elsevier, Amsterdam.

Senoh, S., Creveling, C.R., Udenfriend, S., Witkop, B., 1959. Chemical, enzymatic, and metabolic studies on the mechanism of oxidation of dopamine. J. Am. Chem. Soc. 81**,** 6236-6240.

Senoh, S., Witkop, B., 1959. Non-enzymatic conversions of dopamine to norepinephrine and trihydroxyphenetylamines. J. Am. Chem. Soc. 81**,** 6222-6231.

Shibata, T., Yamada, K., Watanabe, M., Ikenaka, K., Wada, K., Tanaka, K., Inoue, Y., 1997. Glutamate transporter GLAST is expressed in the radial glia-astrocyte lineage of developing mouse spinal cord. J. Neurosci. 17**,** 9212-9219.

Shingo, T., Date, I., Yoshida, H., Ohmoto, T., 2002. Neuroprotective and restorative effects of intrastriatal grafting of encapsulated GDNF-producing cells in a rat model of Parkinson's disease. J. Neurosci. Res. 69**,** 946-954.

Shults, C.W., Hashimoto, R., Brady, R.M., Gage, F.H., 1990. Dopaminergic cells align along radial glia in the developing mesencephalon of the rat. Neuroscience. 38**,** 427-36.

Slevin, J.T., Gerhardt, G.A., Smith, C.D., Gash, D.M., Kryscio, R., Young, B., 2005. Improvement of bilateral motor functions in patients with Parkinson disease through the unilateral intraputaminal infusion of glial cell line-derived neurotrophic factor. J. Neurosurg. 102**,** 216-222.

Spassky, N., Merkle, F., Flames, N., Tramontin, A., Garcia-Verdugo, J., Alvarez-Buylla, A., 2005. Adult ependymal cells are postmitotic and are derived from radial glial cells during embryogenesis. J. Neurosci. 25**,** 10-18.

Specht, L.A., Pickel, V.M., Joh, T.H., Reis, D.J., 1981a. Light microscopic immunocytochemical localization of tyrosine hydroxylase in prenatal rat brain. II. Late ontogeny. J. Comp. Neurol. 199**,** 255-276.

Specht, L.A., Pickel, V.M., Joh, T.H., Reis, D.J., 1981b. Light microscopic immunocytochemical localization of tyrosine hydroxylase in prenatal rat brain. I. Early ontogeny. J. Comp. Neurol. 199**,** 233-253.

Stamford, J.A., 1990. Fast cyclic voltammetry: measuring transmitter release in 'real time'. J. Neurosci. Meth. 34**,** 67-72.

Steece-Collier, K., Collier, T.J., Danielson, P.D., Kurlan, R., Yurek, D.M., Sladek, J.R., Jr., 2003. Embryonic mesencephalic grafts increase levodopa-induced forelimb hyperkinesia in parkinsonian rats. Mov Disord. 18**,** 1442-54.

Stoppini, L., Buchs, P.-A., Muller, D., 1991. A simple method for organotypic cultures of nervous tissue. J. Neursci. Meth. 37**,** 173-182.
Strömberg, I., Johnson, S., Hoffer, B., Olson, L., 1985. Reinnervation of dopamine-denervated striatum by substantia nigra transplants. Immunocytochemical and electrophysiological correlates. Neuroscience. 14**,** 981-998.
Strömberg, I., Almqvist, P., Bygdeman, M., Finger, T., Gerhardt, G., Granholm, A.-C., Mahalik, T., Seiger, Å., Hoffer, B., Olson, L., 1988. Intracerebral xenografts of human mesencephalic tissue into athymic rats: Histochemical and in vivo electrochemical studies. Proc Natl Acad Sci USA. 85**,** 8331-8434.
Strömberg, I., van Horne, C., Bygdeman, M., Weiner, N., Gerhardt, G.A., 1991. Function of intraventricular human mesencephalic xenografts in immunosuppressed rats: an electrophysiological and neurochemical analysis. Exp Neurol. 112**,** 140-52.
Strömberg, I., Bygdeman, M., Almqvist, P., 1992. Target-specific outgrowth from human mesencephalic tissue grafted to cortex or ventricle of immunosuppressed rats. J. Comp. Neurol. 315**,** 445-456.
Strömberg, I., Björklund, L., Johansson, M., Tomac, A., Collins, F., Olson, L., Hoffer, B., Humpel, C., 1993. Glial cell line-derived neurotrophic factor (GDNF) is expressed in the developing but not adult striatum and stimulates developing dopamine neurons in vivo. Exp. Neurol. 124**,** 401-412.
Strömberg, I., Bickford, P., 1996. Reduced aging effects of striatal neuronal discharge rate by aged ventral mesencephalic grafts. NeuroRep. 7**,** 693-696.
Strömberg, I., Björklund, L., Förander, P., 1997. The age of striatum determines the pattern and extent of dopaminergic innervation: A nigrostriatal double graft study. Cell Transplant. 6**,** 287-296.
Surmeier, D.J., Eberwine, J., Wilson, C.J., Cao, Y., Stefani, A., Kitai, S.T., 1992. Dopamine receptor subtypes colocalize in rat striatonigral neurons. Proc. Natl. Acad. Sci. USA. 89**,** 10178-10182.
Takeshima, T., Shimoda, K., Suaves, Y., Commissiong, J.W., 1994. Astrocyte-dependent and -independent phases of the development and survival of rat embryonic day 14 mesencepahlic, dopaminergic neurons in culture. Neurosci. 60**,** 809-823.
Tanaka, H., Kannari, K., Maeda, T., Tomiyama, M., Suda, T., Matsunaga, M., 1999. Role of serotonergic neurons in L-DOPA-derived extracellular dopamine in the striatum of 6-OHDA-lesioned rats. Neuroreport. 10**,** 631-4.
Tennyson, V.M., Barrett, R.E., Cohen, G., Cote, L., Heikkila, R., Mytilineou, C., 1972. The developing neostriatum of the rabbit: correlation of fluorescence histochemistry, electron microscopy, endogenous dopamine levels, and (3 H)dopamine uptake. Brain Res. 46**,** 251-285.
Tissot, R., Bartholini, G., Pletscher, A., 1969. Drug-induced changes of extracerebral dopa metabolism in man. Arch. Neurol. 20**,** 187-190.
Tomac, A., Widenfalk, J., Lin, L.-F.H., Kohino, T., Ebendal, T., Hoffer, B.J., Olson, L., 1995. Retrograde axonal transport of glial cell line-derived neurotrophic factor in the adult nigrostriatal system suggests a trophic role in the adult. Proc. Natl. Acad. Sci. 92**,** 8274-8278.

Törnqvist, N., Björklund, L., Strömberg, I., 2001. Evidence for target-specific outgrowth from subpopulations of grafted dopaminergic neurons. A retrograde study using *in oculo* and intracranial grafting. Exp. Neurol. 169**,** 329-339.
Torres, E.M., Monville, C., Gates, M.A., Bagga, V., Dunnett, S.B., 2007. Improved survival of young donor age dopamine grafts in a rat model of Parkinson's disease. Neurosci. 146**,** 1606-1617.
Tranzer, J.P., Thoenen, H., 1968. An electron microscopic study of selective, acute degeneration of sympathetic nerve terminals after administration of 6-hydroxydopamine. Experientia. 24**,** 155-156.
Trétiakoff, C., 1919. Contribution à l'étude de l'anatomie pathologique du locus niger de Soemmering avec quelques déductions relatives à la pathogénie des troubles du tonus musculaire et de la maladie de Parkinson. Thése Médicine, Paris.
Trupp, M., Scott, R., Whittemore, S.R., Ibanez, C.F., 1999. Ret-dependent and -independent mechanism of GDNF signaling in neuronal cells. J. Biol. Chem. 274**,** 20885-20894.
Ungerstedt, U., 1968. 6-Hydroxydopamine induced degeneration of central monoamine neurons. Eur. J. Pharmacol. 5**,** 107-110.
Ungerstedt, U., Arbuthnott, G.W., 1970. Quantitative recording of rotational behavior in rats after 6-hydroxy-dopamine lesions of the nigrostriatal dopamine system. Brain Res. 24**,** 485-93.
Ungerstedt, U., 1971. Postsynaptic supersensitivity after 6-hydroxydopamine induced degeneration of the nigro-striatal dopamine system. Acta Physiol. Scand. 367**,** 69-93.
van Horne, C., Mahalik, T., Hoffer, B., Bygdeman, M., Almqvist, P., Stieg, P., Seiger, Å., Olson, L., Strömberg, I., 1990. Behavioral and electrophysiological correlates of human mesencephalic dopaminergic xenograft function in the rat striatum. Brain Res Bull. 25**,** 325-334.
van Horne, C., Hoffer, B.J., Strömberg, I., Gerhardt, G.A., 1992. Clearence and diffusion of locally applied dopamine in normal and 6-hydroxydoamine-lesioned rat striatum. J. Pharmacol. Exp. Ther. 263**,** 1285-1292.
Vedas. The four vedas: Rig, Sama, Yajur and Atharva. Vol., ed.^eds.
Voorn, P., Kalsbeek, A., Jorritsma-Byham, B., Groenewegen, H., 1988. The pre- and postnatal development of the dopaminergic cell groups in the ventral mesencephalon and the dopaminergic innervation of the striatum of the rat. Neurosci. 25**,** 857-887.
Wenning, G.K., Odin, P., Morrish, P., Rehncrona, S., Widner, H., Brundin, P., 1997. Short- and long-term survival and function of unilateral intrastriatal dopaminergic grafts in Parkinson's disease. Ann. Neurol. 42**,** 95-107.
Wictorin, K., Ouimet, C.C., Björklund, A., 1989. Intrinsic organization and connectivity of intrastriatal striatal transplants in rats as revealed by DARPP-32 immunohistochemistry: Specificity of connections with the lesioned host brain. Eur. J. Neurosci. 1**,** 690-701.
Winkler, C., Kirik, D., Björklund, A., Cenci, M.A., 2002. L-DOPA-induced dyskinesia in the intrastriatal 6-hydroxydopamine model of Parkinson's disease: relation to motor and cellular parameters of nigrostriatal function. Neurobiol. Dis. 10**,** 165-186.

Yasuhara, T., Shingo, T., Muraoka, K., Kobayashi, K., Takeuchi, A., Yano, A., Wenji, Y., Kameda, M., Matsui, T., Miyoshi, Y., Date, I., 2005. Early transplantation of an encapsulated glial cell line-derived neurotrophic factor-producing cell demonstrating strong neuroprotective effects in a rat model of Parkinson disease. J. Neurosurg. 102**,** 80-89.

Yurek, D.M., Fletcher-Turner, A., 2001. Differential expression of GDNF, BDNF, and NT-3 in the aging nigrostriatal system following a neurotoxic lesion. Brain Res. 891**,** 228-235.

Zarow, C., Lyness, S.A., Mortimer, J.A., Chui, H.C., 2003. Neuronal loss is greater in the locus coeruleus than nucleus basalis and substantia nigra in Alzheimer and Parkinson diseases. Arch. Neurol. 60**,** 337-341.

Zetterström, T., Brundin, P., Gage, F.G., Sharper, T., Isacson, O., Dunnett, S.B., Ungerstedt, U., Björklund, A., 1986. In vivo measurement of spontaneous release and metabolism of dopamine from intrastriatal nigral grafts using intracerebral dialysis. Brain Res. 362**,** 344-349.